MEASUREMENTS OF ABSOLUTE FISSION PRODUCT YIELDS FROM THE THERMAL FISSION OF ^{235}U USING GAMMA-RAY SPECTROSCOPY METHODS

by

Thomas Patrick McLaughlin

A Dissertation Submitted to the Faculty of the

DEPARTMENT OF NUCLEAR ENGINEERING

In Partial Fulfillment of the Requirements
For the Degree of

DOCTOR OF PHILOSOPHY

In the Graduate College

THE UNIVERSITY OF ARIZONA

1 9 7 1

THE UNIVERSITY OF ARIZONA

GRADUATE COLLEGE

I hereby recommend that this dissertation prepared under my direction by Thomas Patrick McLaughlin

entitled Measurements of Absolute Fission Product Yields From the Thermal Fission of ^{235}U Using Gamma-Ray Spectroscopy Methods

be accepted as fulfilling the dissertation requirement of the degree of Doctor of Philosophy

Richard T. Beckm — 9/14/70

Dissertation Director — Date

After inspection of the final copy of the dissertation, the following members of the Final Examination Committee concur in its approval and recommend its acceptance:*

Roald K Wangness	8 September 1970
W J Donahue	8 Sept. 1970
K L Leake	8 Sept. 1970
[illegible]	8 Sept 70
George W Nelson	8 Sept 1970
Gordon E. Hansen	8 Sept 1970

*This approval and acceptance is contingent on the candidate's adequate performance and defense of this dissertation at the final oral examination. The inclusion of this sheet bound into the library copy of the dissertation is evidence of satisfactory performance at the final examination.

STATEMENT BY AUTHOR

This dissertation has been submitted in partial fulfillment of requirements for an advanced degree at The University of Arizona and is deposited in the University Library to be made available to borrowers under rules of the Library.

Brief quotations from this dissertation are allowable without special permission, provided that accurate acknowledgment of source is made. Requests for permission for extended quotation from or reproduction of this manuscript in whole or in part may be granted by the copyright holder.

SIGNED: Thomas P. McLaughlin

To

Thomas V. McLaughlin

ACKNOWLEDGEMENTS

To Dr. Gordon E. Hansen of Los Alamos Scientific Laboratory, for his interest and many helpful discussions throughout the course of this research, the author is sincerely grateful.

The author is also thankful to Dr. Richard L. Brehm of The University of Arizona and Dr. Hugh C. Paxton of Los Alamos Scientific Laboratory for the opportunity to have performed his research at Los Alamos.

In addition, the author would like to express his gratitude to the staff of Los Alamos Scientific Laboratory for the equipment used and assistance given during this work.

TABLE OF CONTENTS

TABLE OF CONTENTS--Continued

LIST OF ILLUSTRATIONS

LIST OF TABLES

ABSTRACT

Calibrated fission foils and a Ge(Li)-NaI Compton-suppressed gamma-ray spectrometer have been used to determine cumulative fission product yields from the thermal neutron fission of ^{235}U. The mass chains 85, 87, 88, 91, 92, 93, 95, 97, 99, 103, 106, 131, 132, 133, 134, 135, 137, 138, 139, 140, 141, 142, 143, 144, 147, and 149 were investigated by observing the gamma-ray spectra from numerous thin ^{235}U samples.

Due to the widely varying decay rates of the fission products, irradiation flux-times were varied to selectively enhance the different full-energy peaks. Half-lives of the useful fission products were in the range, 30 minutes $\leq T_{\frac{1}{2}} \leq$ 30 years, and their prominent gamma-rays in the range, 80 keV $\leq E \leq$ 1600 keV.

This method provides an independent determination of data which was previously obtained by either radiochemical or mass-spectrometric studies. In addition to the speed and convenience of this technique, the accuracy of yield determinations obtained for some mass chains is comparable to that of other methods and the agreement is generally good.

CHAPTER 1

INTRODUCTION

Nuclear fuel burnup determinations are generally based on the measurement of selected fission products present at the end of an irradiation. An important limitation on the accuracy of these calculations is the uncertainty in the fission product yields. In all experimental yield studies the two parameters measured either directly or indirectly are the total number of fissions a sample has undergone and the absolute number of atoms of each fission product of interest.

The absolute number of atoms of each fission product has traditionally been measured by either of two techniques depending on the irradiation history of the sample and the fission products being measured. Isotope dilution mass spectrometry is normally used for determinations of stable and long-lived fission products while radiochemical analysis is usually used for short-lived products.

In the former method, which is the more accurate of the two, determinations of both pre- and post-irradiation sample data are necessary. These data include precise weight percents of the different elements and the isotopic

composition of each element in the sample. In addition, detailed knowledge of the irradiation history and conditions of irradiation are required for accurate capture-to-fission calculations. Careful chemistry is required in the sample dissolution and individual isotope separation to prevent the loss of any fission products. The final step in this method involves precise mass spectrometric analysis by diluting a measured amount of a fission product isotope with a known quantity of another isotope of that same element.

Various methods have been employed for absolute fission determinations. These include fission counting, absolute measurements of the number of fuel atoms before and after irradiation, and the use of flux monitors to measure integrated neutron exposures from which fissions are computed through an appropriate cross-section ratio. In some experiments the number of fissions have not been determined, but the yields are expressed relative to particular fission products. To normalize these relative yields, use is usually made of the requirement that the light and heavy mass groups independently sum to 100%.

Until recently the most accurately known mass chains in the thermal fission of ^{235}U had uncertainties of approximately two percent. A several-year study just completed (Lisman et al. 1969) has reported yields for

most of the prominent mass chains to an accuracy of better than ±1%. Notable omissions in this tabulation were values for mass numbers 135 and 136, due to the large uncertainties in the burnup of ^{135}Xe and mass 103 due to the relatively short half-life of ^{103}Ru. Isotope dilution mass spectrometry of the stable fission products was the principal measurement technique used in this study.

The development of high resolution germanium lithium-drifted, Ge(Li), detectors has opened up a third major approach to fission product analyses. Although this method is applicable primarily to nuclides with yields greater than one percent that decay with significant gamma emission, the results may be combined with those from mass spectrometric studies to give excellent over-all yield determinations. The accuracy of absolute yield determinations made by Ge(Li) spectroscopy is currently limited by uncertainties in gamma-ray intensities and/or the detector efficiency calibration.

Gordon, Harvey, and Nakahara (1966) used a planar Ge(Li) detector to determine 18 yields, all with half-lives greater than one hour, from the thermal fission of ^{233}U. This was accomplished by comparing the delayed gamma spectra of ^{233}U and ^{235}U and then estimating the ^{233}U yields based on the literature values of the better-known ^{235}U yields. Short-lived Ge(Li) gamma spectra from the thermal fission

of ^{235}U (Boggs 1966) and the fast fission of ^{239}Pu (Moore 1969) have also been reported. In both studies half-lives between approximately one minute and one hour were determined for prominent full-energy peaks; however, only in the latter experiment were yield estimates made for various short-lived fission products. Recent investigations of the gross gamma spectra for both ^{235}U and ^{239}Pu (Murri and Heath 1968) have been made for times between 3 hours and 500 days after irradiation. The Ge(Li) spectra were analyzed mainly for the purpose of full-energy peak identification.

CHAPTER 2

MEASURING ABSOLUTE CHAIN YIELDS

Although work on cumulative mass yield determinations using gamma ray spectroscopy techniques has been proceeding since 1965, all such research has relied on mass spectrometric and/or radiochemically determined yields for normalizing the results. The reason for this was the inability to accurately obtain a small sample having only 10^{10} to 10^{13} fissions. The samples used for quantitative detection of gamma-rays must be axially thin to minimize errors due to source self-absorption of gamma-rays. Further, these samples must be approximately the same size radially as the sources used in the detector efficiency calibration. Mass spectrometric studies, however, require of the order of 10^{20} fissions in a sample containing several grams of fissile material to enable an accurate determination of the total number of fissions.

With the aid of calibrated fission foils, an ionization chamber, and a suitable reactor flux it is a relatively straightforward procedure to submit a sample to an accurately measurable number of fissions.

Fission Counting

Calibrated fission foils have been in existence in the Radiochemistry Group, J-11, at Los Alamos Scientific Laboratory for many years. Available are foils with deposits of ^{235}U or ^{239}Pu with masses ranging from about 0.01 to 100.0 micrograms. The uncertainty in the mass of each fissile deposit is stated as ± 1.0% (Knobeloch 1965).

Consider a fission foil containing a mass, M_1, of pure ^{235}U deposited on a flat backing material, placed in a 2π ionization chamber and thence subjected to a suitable neutron flux. If the fissile deposit is very thin and uniform, then each fission event will result in the ejection of one fission fragment into the chamber and its subsequent detection. These events are then recorded with appropriate instrumentation. Thus a 2π ionization chamber can be an absolute fission monitor for foils in which self-absorption is negligible.

Next, place a second mass, M_2, also of pure ^{235}U behind the fission foil, and hence outside the sensitive volume of the chamber. For identical fluxes throughout both M_1 and M_2, the number of fissions per second occurring in M_2 is

$$R_2 = \left(\frac{M_2}{M_1}\right) R_1 \qquad (2\text{-}1)$$

where R_1 is the rate of fission events in M_1. Since M_2 will

typically weigh of the order of milligrams, the flux in both M_1 and M_2 is depressed relative to the unperturbed flux. Then, for different fluxes in M_1 and M_2, the right-hand side of Equation (2-1) must be multiplied by the ratio of the average flux in M_2 to the average flux in M_1.

Independent, Cumulative, and Total Chain Yields

The fission process produces a distribution of primary products for each mass chain. Based on the latest correlation of available data (Wahl et al. to be published) the charge distributions of the isobars for each mass chain are seemingly best fit by Gaussian functions. Mass 134 is an exception to this correlation.

The probability per fission that a particular nuclide will be formed directly, and not as the result of the decay of another member of that mass chain, is known as the independent yield of that nuclide. The cumulative yield of a fission product is the probability per fission that the fission product is formed either directly or later in the decay chain. Total chain yield is in nearly all instances equivalent to the cumulative yield of the last decaying member of a mass chain. Independent yields of stable isotopes are much less than the total uncertainties associated with each cumulative yield determined in this experiment.

Delayed Gamma-Ray Emission

Fission product gamma-rays emanate from the radioactive nuclides formed by the fission process. Primary fission fragments, generally having too many neutrons for stability, decay most often by electron emission and only infrequently by neutron emission. As a primary fragment successively beta decays toward a stable isotope, each daughter isotope is frequently formed in an excited state with gamma-ray emission being the most probable de-excitation mode.

The delayed gamma-ray spectrum will be determined mainly by those fission products having both considerable gamma-ray emission per decay and high independent or cumulative yields. The relative prominence of a particular full-energy peak present in a gamma spectrum is also dependent on the half-lives of the fission products and the time after irradiation at which the gamma spectrum is collected. This is illustrated in Appendix B where spectra taken at approximately three hours, one day, one week, and eight weeks after irradiation are presented. At a particular time, t_1, after irradiation, those full-energy peaks most enhanced emanate from radionuclides whose half-lives are of the order of t_1. At this time the decay of the shorter-lived nuclides will have reduced their specific activity below those of interest while longer-lived species will

always have relatively low specific activities.

For all mass numbers considered, accurate independent yield data were not a prerequisite to determining the cumulative chain yields accurately. The half-lives of isobars with significant independent yields prior in the decay chain to the radionuclide of interest were, in most cases, sufficiently short that the cumulative yield of the long-lived isotope could be interpreted as an independent yield for purposes of radioactive decay calculations. This simplified calculations to the point that the full-energy counts for all gamma-rays of interest could be assumed to have begun with either a single radionuclide decay or a daughter decay with one parent. The full-energy counts of a particular gamma-ray detected in a counting interval from a single decay are

$$C = Yp\left(\frac{\epsilon I_\gamma f_{SA} T_L}{t_1 \lambda}\right)\left(1-e^{-\lambda t_1}\right) e^{-\lambda(t_2-t_1)} \left(1-e^{-\lambda(t_3-t_2)}\right). \quad (2\text{-}2)$$

The corresponding equation for a daughter decaying from one parent is

$$C = Yp\left(\frac{\epsilon I_\gamma f_{SA} T_L}{t_1}\right)\left[\left(\frac{\lambda_2}{\lambda_1(\lambda_2-\lambda_1)}\right)\left(1-e^{-\lambda_1 t_1}\right)\left(e^{-\lambda_1(t_2-t_1)} - e^{-\lambda_1(t_3-t_1)}\right) - \frac{\lambda_1}{\lambda_2(\lambda_2-\lambda_1)}\left(1-e^{-\lambda_2 t_1}\right)\left(e^{-\lambda_2(t_2-t_1)} - e^{-\lambda_2(t_3-t_1)}\right)\right] \quad (2\text{-}3)$$

where

C is the number of full-energy events of a particular gamma-ray detected in the counting interval,

Y is the cumulative yield of the fission product emitting the gamma-ray,

P is the number of fissions,

ϵ is the probability of the detector recording a full-energy event per gamma-ray emitted from the source; the absolute full-energy peak efficiency,

I_γ is the probability of a particular gamma-ray being emitted per beta decay,

f_{SA} is the probability that a gamma-ray will leave the source without any interactions,

T_L is the fraction of the time in which the detection system is able to accept pulses, the live time,

t_1 is the length of time the sample was irradiated,

t_2 is the time when counting of the sample began,

t_3 is the time when counting of the sample stopped,

λ_1 is the decay constant of the parent, and

λ_2 is the decay constant of the gamma-emitting nuclide, the daughter.

All times are relative to time zero, the time the irradiation began. Equations (2-2) and (2-3) are derived in Appendix D.

Due to various experimental factors, not all of the desired gamma-ray full-energy peaks could be accurately obtained from samples irradiated in the ionization chamber. These additional full-energy peaks were determined through irradiation of the ^{235}U samples in higher thermal fluxes. For example, suppose that full-energy peaks 1 and 2 are very prominent in the spectrum from Sample A which had undergone an unknown number of fissions. Furthermore, let full-energy peak 2 also be pronounced in the gamma spectrum from Sample B which had undergone an accurately measured number of fissions. Then the absolute cumulative yield of the nuclide giving rise to full-energy peak 1 is

$$Y_1 = \frac{C_1}{C_2} Y_2 \frac{I_{\gamma 2} f_{SA2} \epsilon_2}{I_{\gamma 1} f_{SA1} \epsilon_1} \frac{D_1}{D_2} \qquad (2\text{-}4)$$

where D_1 and D_2 are the decay factor terms from Equations (2-2) and/or (2-3), whichever is applicable. Equation (2-4) applies to Sample A, thus C_1, C_2, t_1, t_2, and t_3 are relevant to Sample A only. The role which Sample B plays is only in determining Y_2. Gamma-ray detection system dead time measurements are unnecessary when counting these relative samples.

Equations (2-2), (2-3), or (2-4) do not account for possible neutron decay or isomeric branching. Although neutron decay only occurs among short-lived fission products and is not a factor in applying the decay equations to the data of this experiment, it should be considered when detecting gamma-rays from short-lived nuclides, in particular bromine and iodine fission products. Isomeric branching is generally a much more significant effect than neutron decay and does occur for some of the decay products observed in this experiment. However, accounting for this latter effect is straight-forward if the branching ratio and half-lives are well known.

Delayed Gamma-Ray Detection

A detector with excellent energy resolution is clearly a necessity for resolving individual gamma-ray, full-energy peaks from gross fission spectra. The lithium drifted germanium, Ge(Li), detector fulfills this requirement over a broad energy range. As this detector has been the subject of numerous reports only a brief description of its construction and operation will be given here.

The starting material for the Ge(Li) detector is p-type germanium (germanium doped typically with gallium). Lithium which acts as a donor is diffused at approximately 400°C into the surface making the germanium n-type in these surface regions. To obtain an intrinsic or electrically

neutral region between the p-type and n-type regions, which will enable the collection of free charges, the lithium ions are then drifted inward by an applied bias voltage. The undrifted portion of the detector is still p-type and thus the detector becomes a simple p-i-n junction semiconductor device.

Ge(Li) detectors are operated at liquid nitrogen temperatures for two main reasons. First, the mobility of the lithium is essentially zero at this temperature, maintaining the p-i-n structure indefinitely. Second, as germanium has a narrow band gap energy, operation in this temperature regime minimizes thermal noise and enables the use of very low noise field-effect transistor, FET, preamplifiers. To a large extent the observed full width at half maximum, FWHM, for a gamma-ray is determined by the contributions due to the preamplifier noise and the detector capacitance. To a much lesser degree the shaping time constants of the main amplifier influence resolution. The over-all system resolution, expressed as FWHM, is then given by

$$FWHM = \left[FWHM_{det}^{2} + FWHM_{el}^{2} \right]^{\frac{1}{2}} \qquad (2\text{-}5)$$

where $FWHM_{det}$ is the detector contribution and $FWHM_{el}$ is the electronics contribution.

For gamma-rays with energies between 80 keV and 1.6 MeV, the photoelectric effect and Compton scattering are the major interaction processes in germanium. Above 150 keV Compton scattering predominates over the photoelectric effect in germanium. Thus when detecting gross fission product gamma-ray spectra, the partial absorption of gamma-rays can create a background which completely masks low energy, low intensity gamma-rays. This background causes full-energy peak integrations to be less accurate even for the prominent low energy peaks.

The large volume (50-75 cm^3) of current Ge(Li) detectors has aided significantly in reducing the loss of Compton scattered gamma-rays. The ratio of the full-energy peak height to Compton edge with current detectors now approaches 20 to 1 for 1.0 MeV gamma-rays. Independent of the size and characteristics of a particular Ge(Li) detector, there is another method for further suppressing the Compton continuum. Surrounding the Ge(Li) detector with a high efficiency detector such as sodium iodide, NaI, will enable detection of most of the scattered gamma-rays which escape the central detector. The NaI signal can thus be used to disable the multichannel analyzer and prevent many of the partial energy pulses occurring in the Ge(Li) detector from being recorded. Using this method of Compton suppression, full-energy peak to Compton edge ratios greater than 100 to

1 have been obtained. Therefore, a large Ge(Li) detector in conjunction with a large NaI detector will greatly facilitate the study of gross fission product gamma-ray spectra.

Another requirement of a detection system for studying gamma-rays over a broad energy band is a large multichannel analyzer. An example will best illustrate this need. For accurate peak integration several channels are necessary to define a full-energy peak above FWHM. If the energy range spans 2000 keV and the detector resolution is 3 keV, then a 4096 channel analyzer has available approximately 6 channels to define a peak. This was sufficient for the computer code used in the gamma-ray spectra analyses of this experiment.

CHAPTER 3

EXPERIMENTAL PROCEDURE

Due to the number and diversity of independent topics covered in this chapter, an outline of the over-all procedure will be given first.

Fission foils prepared for this experiment were calibrated by absolute fission counting against foils of accurately known masses in a double-sided ionization chamber (Knobeloch 1965). Several small disc-shaped samples of ^{235}U were then irradiated in either the Water Boiler Reactor or Omega West Reactor at Los Alamos Scientific Laboratory. Those samples irradiated in the Water Boiler Reactor had previously been accurately weighed and were used as standards. These standard samples were separately irradiated in the ionization chamber, each in the presence of a calibrated fission foil. Thus by the method described in Chapter 2 a measured number of fissions were induced in each of the standard samples. After appropriate cooling times to enhance the gamma-ray peaks of interest, the samples were placed in a reproducible geometry and each counted several times. Data obtained from samples irradiated in the Omega West Reactor were normalized to the standard sample data by comparison of full-energy peaks in

the gamma-ray spectra. Start and stop times for all sample irradiations and for all gamma-ray counting intervals were accurately recorded. When gamma counting the standard samples, dead time measurements were also made.

The efficiency of the Ge(Li) detector was determined with the aid of calibrated gamma-ray sources and, to a lesser extent, uncalibrated sources which have known relative intensities.

Fission Foil Calibrations

For this experiment three fission foils of approximately 36 nanograms of ^{235}U each were prepared by a vacuum evaporation technique in Group CMF-4 of the Los Alamos Scientific Laboratory (Povelites 1965). This deposition technique produces a very uniform layer of material over an accurately known area. The uranium was deposited on a 4.77-cm-diameter by 0.127-mm-thick high purity platinum disc in each case. The deposit itself was 6.35 mm in diameter and was centered on the platinum disc.

The isotopic composition of this uranium is given in Table 1. Uncertainties in the listed weight percents were stated as: ^{234}U and ^{236}U - 3.0%, ^{238}U - 1.0%, and ^{235}U - 0.1% (Tisinger 1970).

Table 1. Isotopic composition of fission foil uranium

ISOTOPE	ATOM %	WEIGHT %
^{234}U	1.03	1.02
^{235}U	93.25	93.19
^{236}U	0.26	0.26
^{238}U	5.44	5.51

The calibration of these foils was performed by fission counting against one calibrated fission foil of nearly identical mass and against two other calibrated fission foils of masses about a factor of two greater. The neutron flux used for fission counting is that found in a thermal column of the Los Alamos Water Boiler Reactor. The flux is approximately $(1.5)10^{10}$ neutrons/cm^2-sec at a maximum power of 25 kW, with a cadmium ratio of about 40 to 1 based on indium.

The foil to be calibrated and a standard were inserted into the double-sided ionization chamber and two counts each totaling at least 300,000 fissions per foil were taken. The chamber was then withdrawn from the reactor and the two foils were interchanged and rotated 180° with respect to each other before two more counts were taken. The average of all four counting ratios was taken to represent the ratio of the masses of ^{235}U on the foils. The 180° rotation and averaging of the four counting ratios insured that any effects due to coupling of chamber flux

gradients with radial or circumferential asymmetries in the fissile deposits would be canceled.

An experimental verification that chamber flux gradients were small was performed. A small amount of ^{235}U deposited on platinum about 3.0 mm in diameter was first positioned at the center of a platinum disc identical to the ones used for fission foils. A count was taken at this position and then the fissile deposit was moved out along a radius to two other positions. At both of these radial locations counts were taken at four angular positions 90° apart by rotation of the 4.77-cm-diameter platinum foil after each count. Results of this investigation are shown in Figure 1.

The electronics for this counting system are very simple. The signal from each side of the counter is fed in parallel to dual sets of preamplifiers, amplifiers, and scalers. The signal from any amplifier may also be fed to a 200-channel pulse height analyzer where the energy spectrum of the fission fragments may be examined. The response of the ionization chamber to one of the 36 nanogram ^{235}U foils calibrated in this experiment is shown in Figure 2.

The ionization chamber dead time has previously been measured and is about 3 microseconds. Thus at the counting rates of 40,000 cpm and below used in the experiment there are no appreciable dead time corrections.

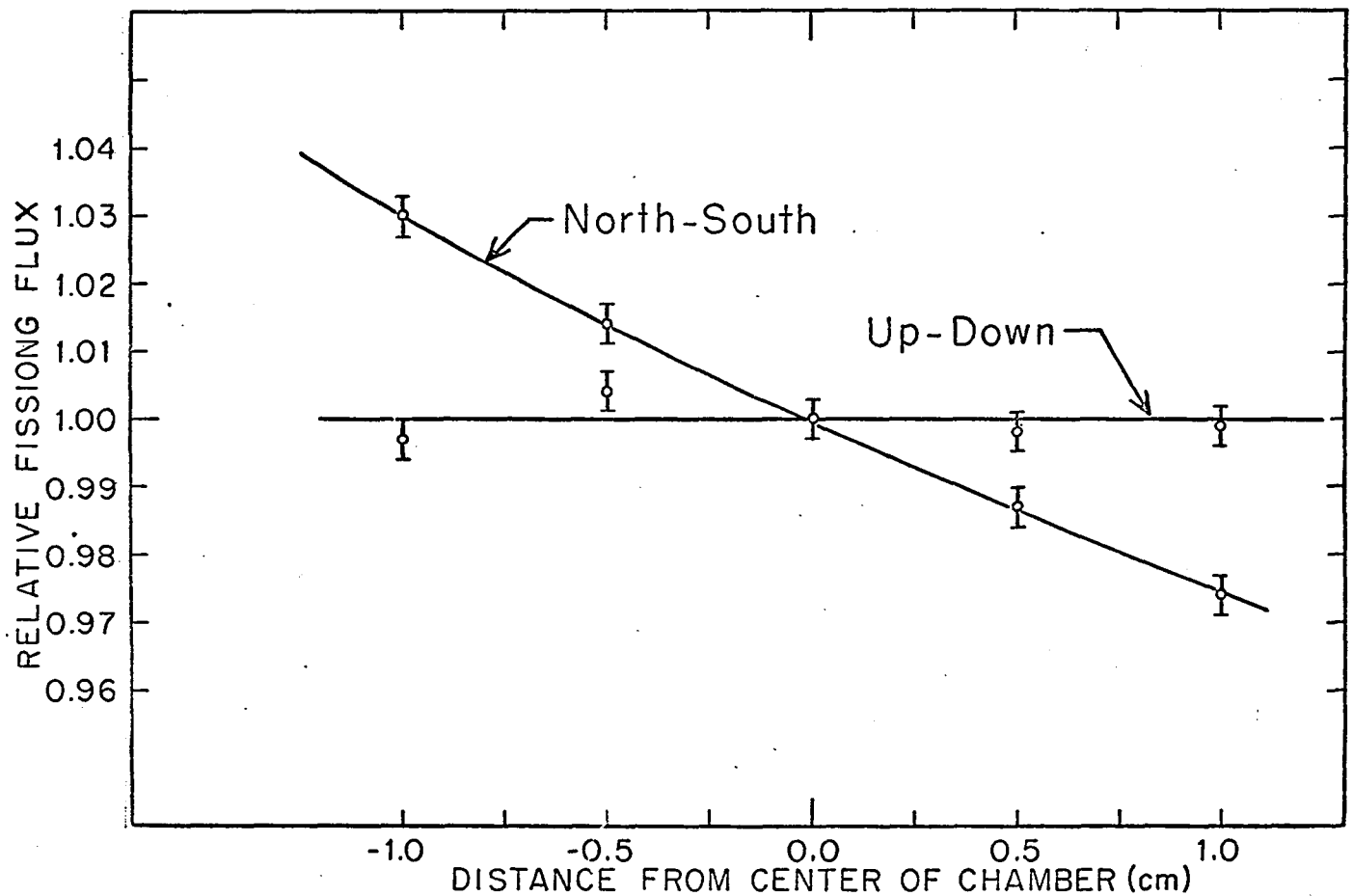

Fig. 1. Fission chamber flux gradients.

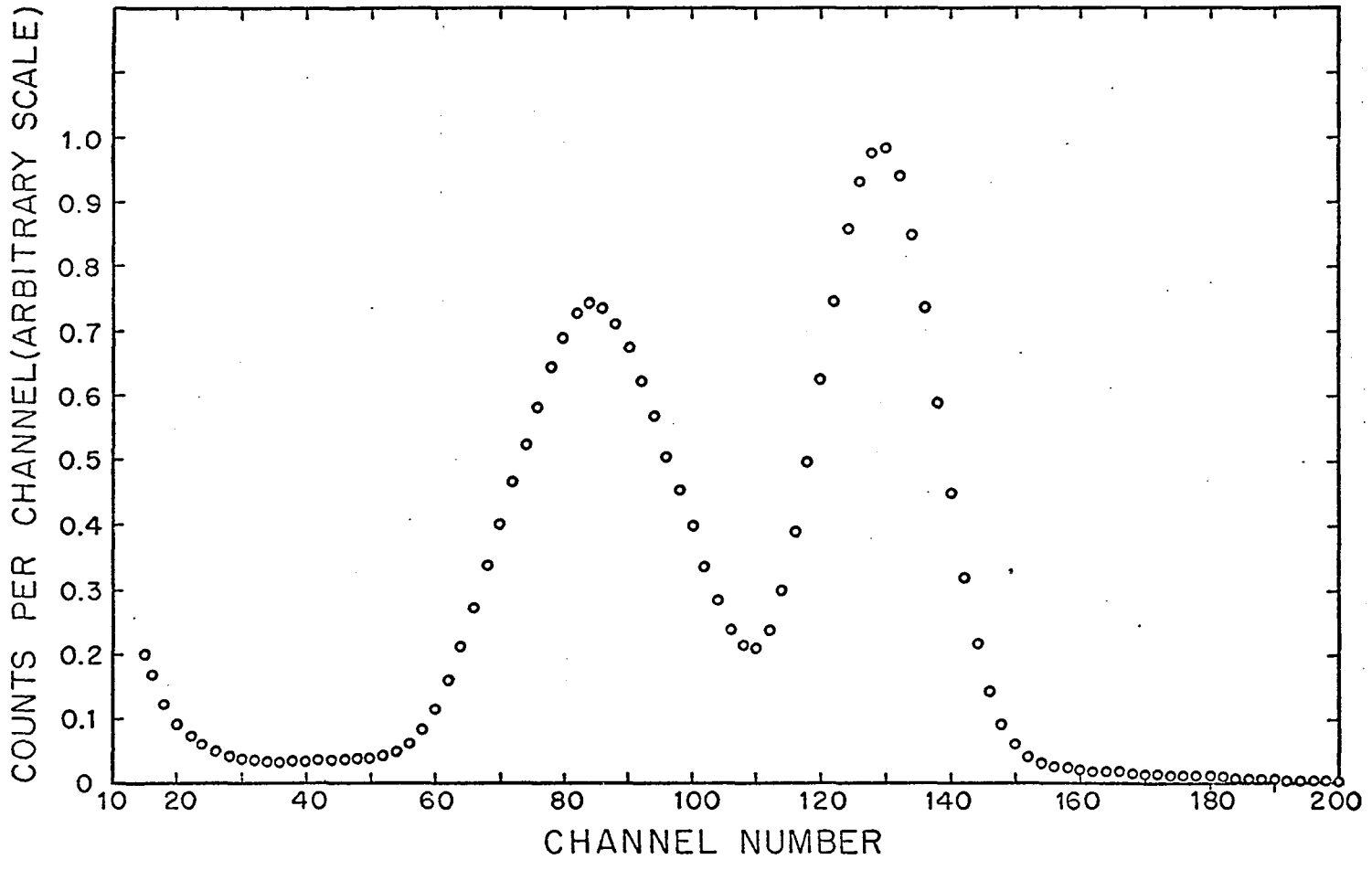

Fig. 2. Fission fragment spectrum from 36 nanogram ^{235}U deposit.

^{235}U Samples

Many factors were considered before deciding upon the dimensions of the ^{235}U samples to be used in this experiment. Flux depression considerations dictated that the samples be as thin as possible. This is because the energy dependent flux had not been measured at the irradiation position, making any flux depression calculations only approximate. Although gamma-ray self-absorption in the sample was of lesser importance, it too would be minimized by using thin samples. The source-to-detector distance and physical arrangement of the Ge(Li) and NaI detectors made it desirable to have the diameters of the samples also a minimum. The rate at which fissions could be induced in a standard sample was determined entirely by the mass of the sample and the maximum flux obtainable at the location of the ionization chamber. To prevent irradiation times of more than several hours at the maximum reactor power level, a minimum value of the mass of a standard sample of about 15 milligrams was obtained from preliminary calculations. From these considerations and the availability of ^{235}U foil, sample dimensions of 6.35 mm in diameter by 0.025 mm thick were decided upon. In all, 24 samples were punched from uranium foil whose isotopic composition is the same as that given in Table 1 for the fission foils.

Prior to weighing of the three ^{235}U samples which were to be used as standards and irradiated in the ionization chamber, they were cleaned in a dilute nitric acid solution. This avoided any weighing errors due to UO_2 and U_3O_8 buildup on the surfaces. Weighing was done in Group CMB-1 of the Los Alamos Scientific Laboratory and the uncertainty in the mass of each standard sample was stated as ± 30 micrograms or about ± 0.2%.

Reactor Irradiations

Irradiations of the ^{235}U samples were performed in either the Water Boiler Reactor or Omega West Reactor. The ionization chamber employed for both fission foil calibrations and standard sample irradiations was set up to be used only in a thermal column of the Water Boiler Reactor. The maximum flux at this position in the thermal column was not sufficient to enable a 15-mg sample to undergo the necessary fissions to permit accurate detection of gamma-rays from fission products with half-lives greater than about 15 days. Also, short-lived activation in the platinum present in the standard sample irradiation geometry prevented accurate data analysis of gamma-ray full-energy peaks from fission products with half-lives less than about 10 hours. This platinum activation caused both large dead times and many interfering peaks at short times after irradiation.

The three standard samples were each irradiated once for 30 minutes and then two of these samples were further irradiated for about 5 hours each. After each 30-minute irradiation the samples were gamma counted twice with each counting interval being about 10 hours and the first count beginning approximately 8 hours after irradiation. Half-lives between about 10 hours and 3 days were obtained from these data. Between the 30-minute and 5-hour irradiations extreme care was taken in order not to compromise the fissile deposit. From the 5-hour data half-lives between 3 days and 15 days were obtained.

Irradiations in the Omega West Reactor were performed in the thermal column rabbit and varied from one minute to twenty minutes. The flux obtainable was about two orders of magnitude greater than that in the ionization chamber. The one-minute irradiations enabled spectra to be taken as early as 3 hours after irradiation and the 20-minute irradiations induced sufficient activity for spectra to be taken after 8 weeks. All relative sample irradiations were performed in duplicate and the results averaged.

The physical arrangement of the ^{235}U samples for the Omega West Reactor irradiations was a sandwich consisting of three disc-shaped layers of 0.076 mm thick aluminum foil with a 6.35-mm-diameter hole cut out of the middle layer of aluminum for positioning the sample. A fast-drying

plastic cement which could be applied in very thin and uniform layers fastened the sandwich together. For irradiation of the standard samples each ^{235}U sample was cemented directly to the back of a platinum fission foil. Here only two aluminum discs were required, again one had a 6.35-mm hole for centering the sample and the other was solid to prevent fission fragments from escaping. Cementing the ^{235}U samples directly to the back of the platinum fission foils minimized the flux difference between that at the fissile deposit and the average in the sample. The aluminum foil thickness of 0.076 mm was chosen for two reasons. First, the range of the most energetic ^{235}U fission fragments is approximately 0.025 mm in aluminum; and, second, gamma-ray attenuation through this thickness of aluminum is negligible at all energies of interest in this experiment.

A blank aluminum sandwich was also irradiated to check on possible interfering peaks either from aluminum or its impurities or from the plastic cement. Count rates were barely above background even at short times after irradiation and no significant peaks were observed.

Gamma-Ray Detection System

Primary gamma-ray detection was performed by a closed-ended coaxial Ge(Li) detector of about 50 cm^3 active volume. The system resolution with this detector was 2.8 keV FWHM for the 1.33 MeV gamma-rays from ^{60}Co. Compton suppression was performed by a NaI annulus surrounding the Ge(Li) detector. This anticoincidence mantel was 20.3 cm in diameter by 30.5-cm long, with an inside diameter of 7.6 cm. Lead shielding, 15.2-cm thick, surrounded the NaI detector on all sides except for holes at both ends. Source gamma-rays were collimated through one hole while the other accommodated the cryostat extension housing the Ge(Li) detector. The source-detector distance was about 95 cm. This source-detector configuration is shown schematically in Figure 3.

Gamma-rays from the source were collimated by a two-section removable lead collimator. The collimator was designed to permit all gamma-rays from a 6.35-mm-diameter disc source a direct path to the total front surface area of the cryostat containing the Ge(Li) detector. Although this design allowed some direct radiation to interact with the NaI crystal, counting rates were always less than those of the Ge(Li) detector.

For quantitative research, especially with a coaxial type Ge(Li) detector, this collimator design is a necessity.

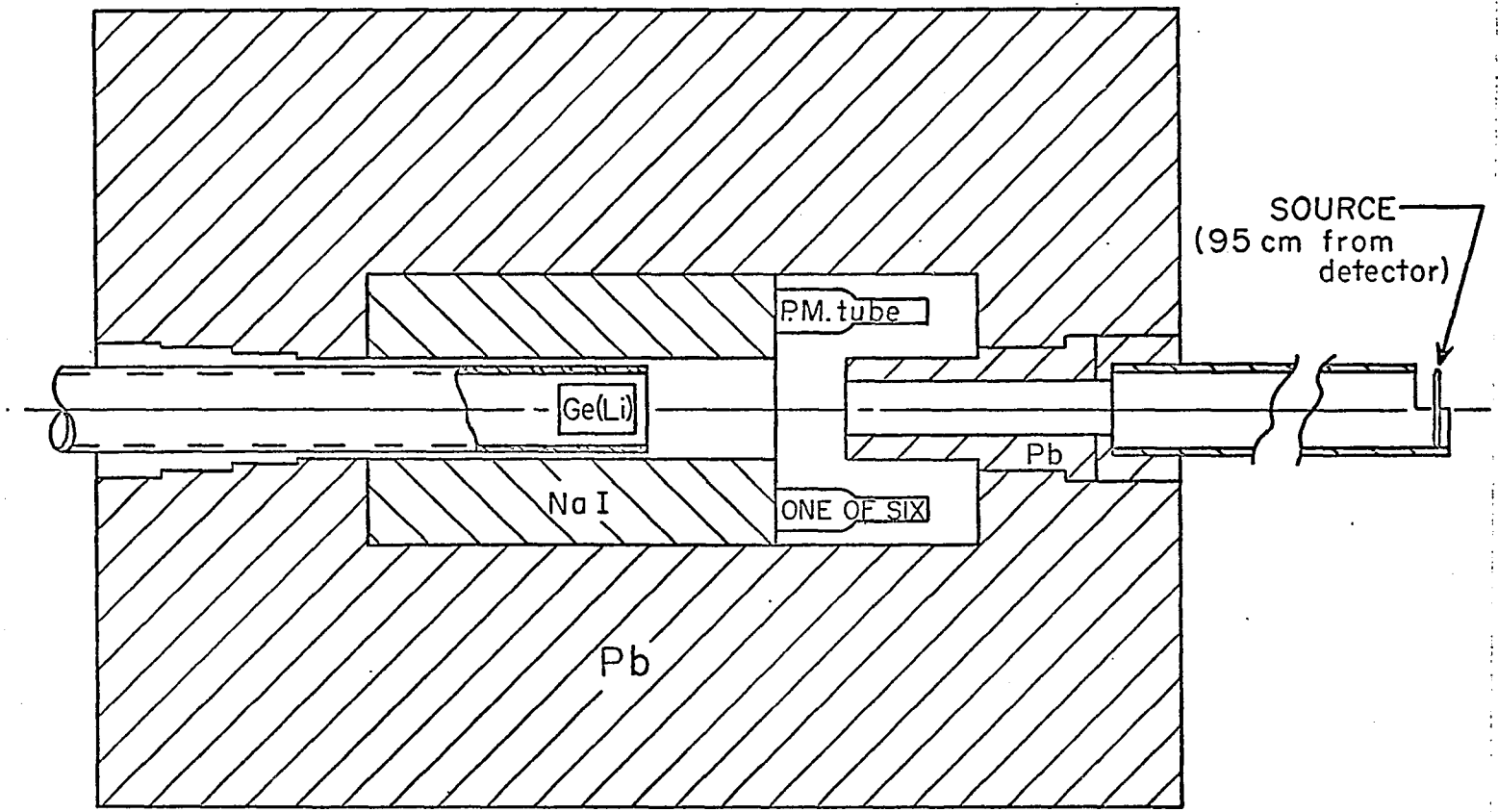

Fig. 3. Source-detector geometry.

Experiments with very finely collimated gamma-ray beams (Malm 1966) have shown that the full-energy peak efficiency varies greatly over the surfaces of these detectors. Therefore, if the collimator prevented any source gamma-rays from having a direct path to the Ge(Li) detector, a meaningful efficiency calibration would be impossible.

The NaI annulus was used in anticoincidence with the Ge(Li) detector to suppress the Compton contribution from scattered gamma-rays. The output of the six photomultiplier tubes associated with the NaI detector were summed and this signal was used to momentarily disable the multichannel analyzer. Illustration of the effectiveness of this method for reducing the Compton distribution is given in Figures 4 and 5. Figure 4 shows a typical ^{60}Co spectrum without Compton suppression and Figure 5 shows a similar ^{60}Co spectrum with Compton suppression. As can be seen from the figures, the full-energy peak height to Compton edge ratio for the 1.33-MeV peak has been increased from 19 to 1 to about 70 to 1 for this detector arrangement.

When counting the standard ^{235}U samples accurate knowledge of the system dead time was required. As the Ge(Li) count rates for all standard sample counts were always less than 400 counts per second, dead time was associated entirely with the multichannel analyzer. A digital clock situated directly above the analyzer was used

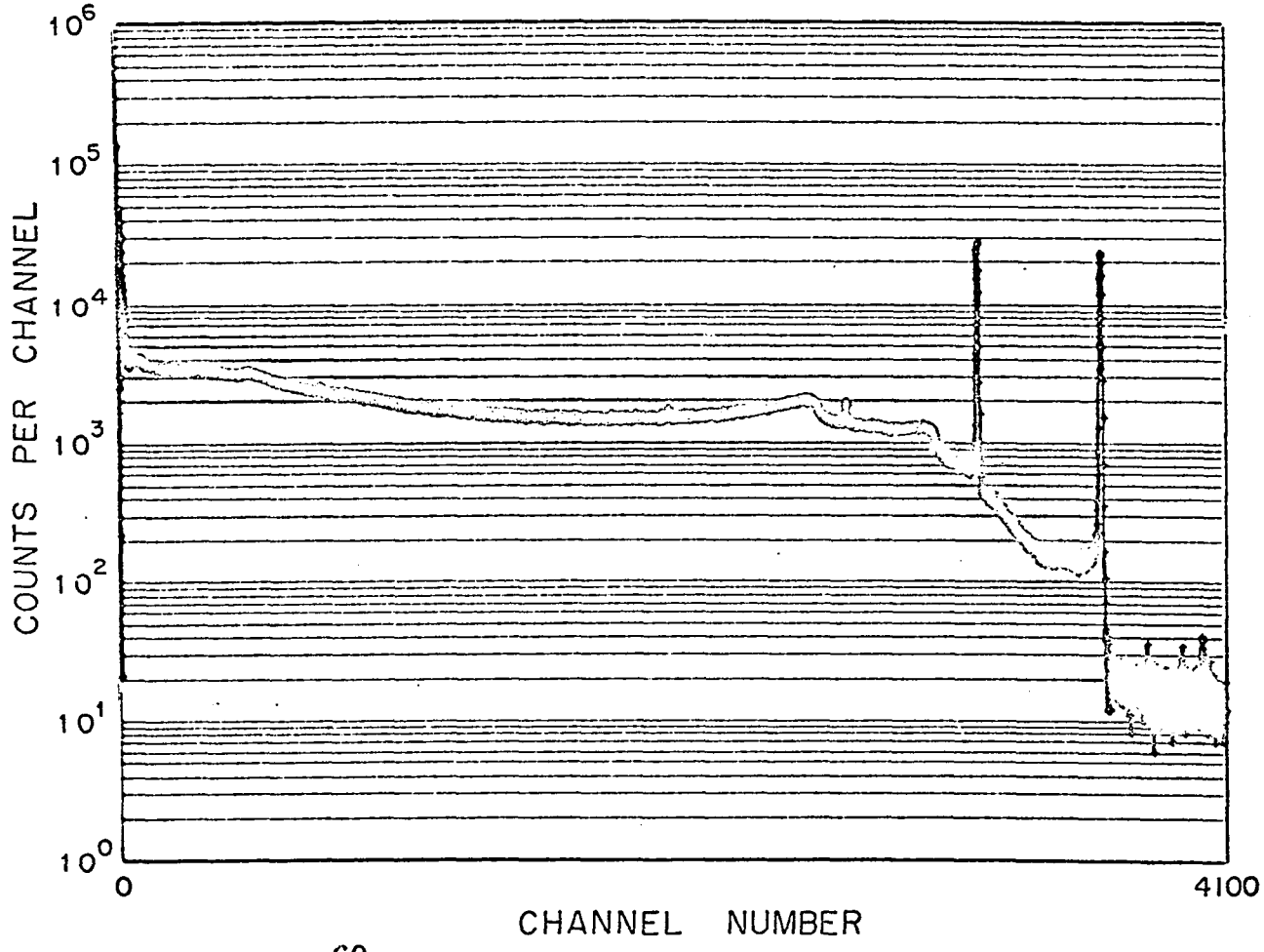

Fig. 4. ^{60}Co spectrum without Compton suppression.

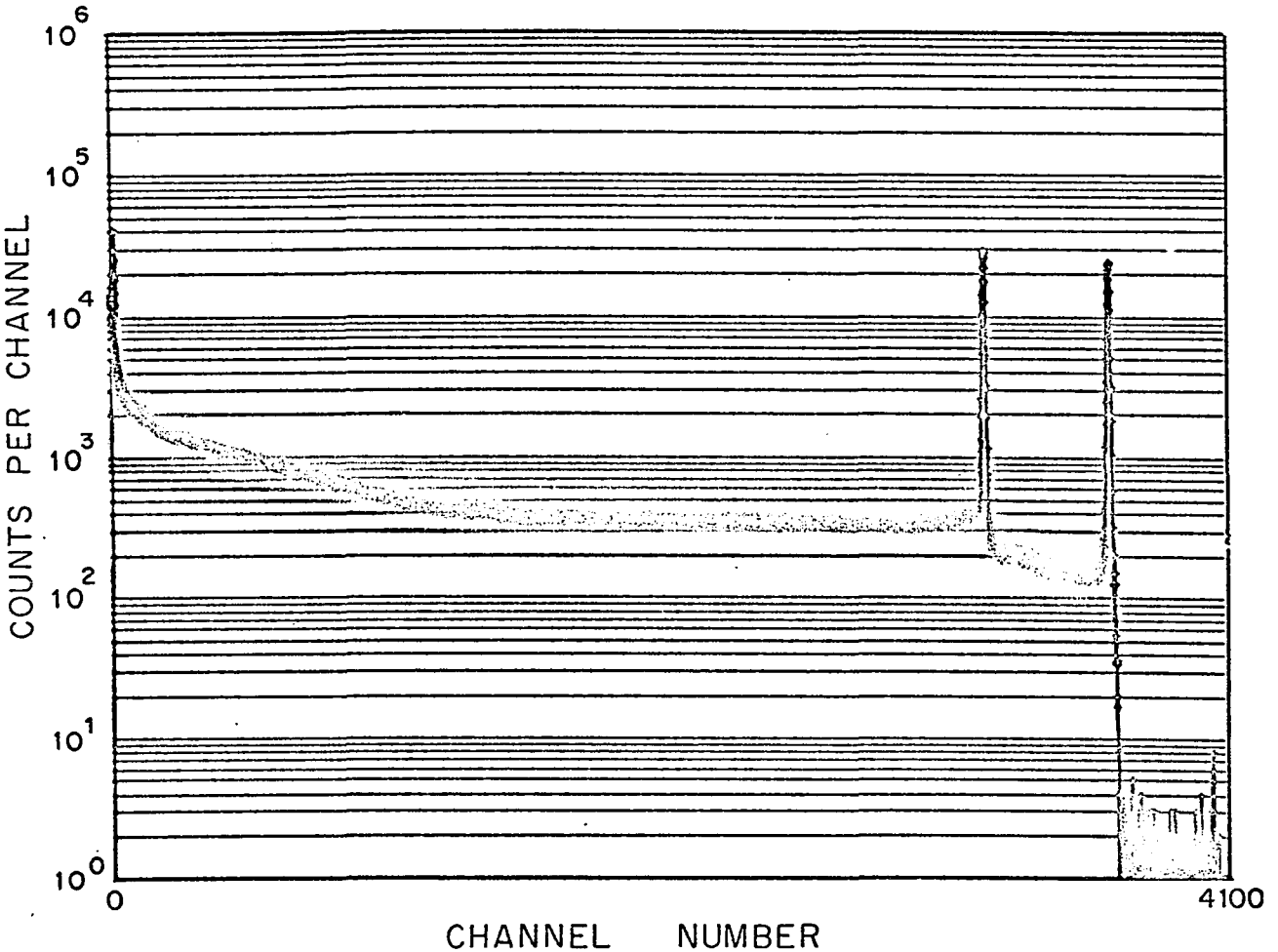

Fig. 5. ^{60}Co spectrum with Compton suppression.

for the dead time corrections in the following manner. With a sample mounted in the source holder and the analyzer set to count in the live-time mode for 10 minutes, the clock times at which the analyzer started and stopped counting were recorded. The amount by which this clock time interval exceeded 10 minutes was then taken as the dead time for that 10-minute counting interval. This procedure was repeated before and after each count of a standard sample was taken. Dead times measured for the standard sample counts ranged from a maximum of 2.3% to a minimum of 0.33% using this technique. With no sample in the source holder there was no measurable dead time.

Instrumentation System

The Ge(Li) signal was first fed through a Canberra model 1408C spectroscopy preamplifier and then through the main amplifier, a Canberra model 1417B. This amplifier has pole-zero cancellation and a baseline restorer on its output. The amplifier signal was then sent to the 4096 channel analyzer, Nuclear Data model 160M.

The signal from the output of the photomultiplier tubes was amplified first by a LASL model 225V preamplifier and then by a LASL model 8021 main amplifier. This pulse was then sent through a LASL model 204 coincidence unit to stretch and delay the pulse sufficiently to insure that the

NaI anticoincidence pulse overlapped the corresponding Ge(Li) pulse.

After each counting interval the contents of the memory of the analyzer were transferred to magnetic tape together with an appropriate identification. The instrumentation system is shown in block diagram form in Figure 6.

Ge(Li) Efficiency Calibration

Absolute full-energy peak efficiency is defined in this paper as the ratio of the number of gamma-rays seen as full-energy events by the detector to all gamma-rays of that energy emitted by the source. This efficiency is then a function of the source-detector distance and alignment, requiring that all data be taken in the same source-detector geometry.

A 1970 set of calibrated International Atomic Energy Agency, IAEA, gamma-ray standards were the primary calibration sources. In addition, sources of ^{166m}Ho, ^{154}Eu, and ^{133}Ba having accurately measured relative gamma-ray intensities and at least one gamma-ray very close in energy to an IAEA calibration standard were available. Thus, measurements of gamma-ray spectra from sources of ^{166m}Ho, ^{154}Eu, and ^{133}Ba, taken in the standard geometry and normalized to the IAEA standards, aided in establishing the shape of the efficiency curve.

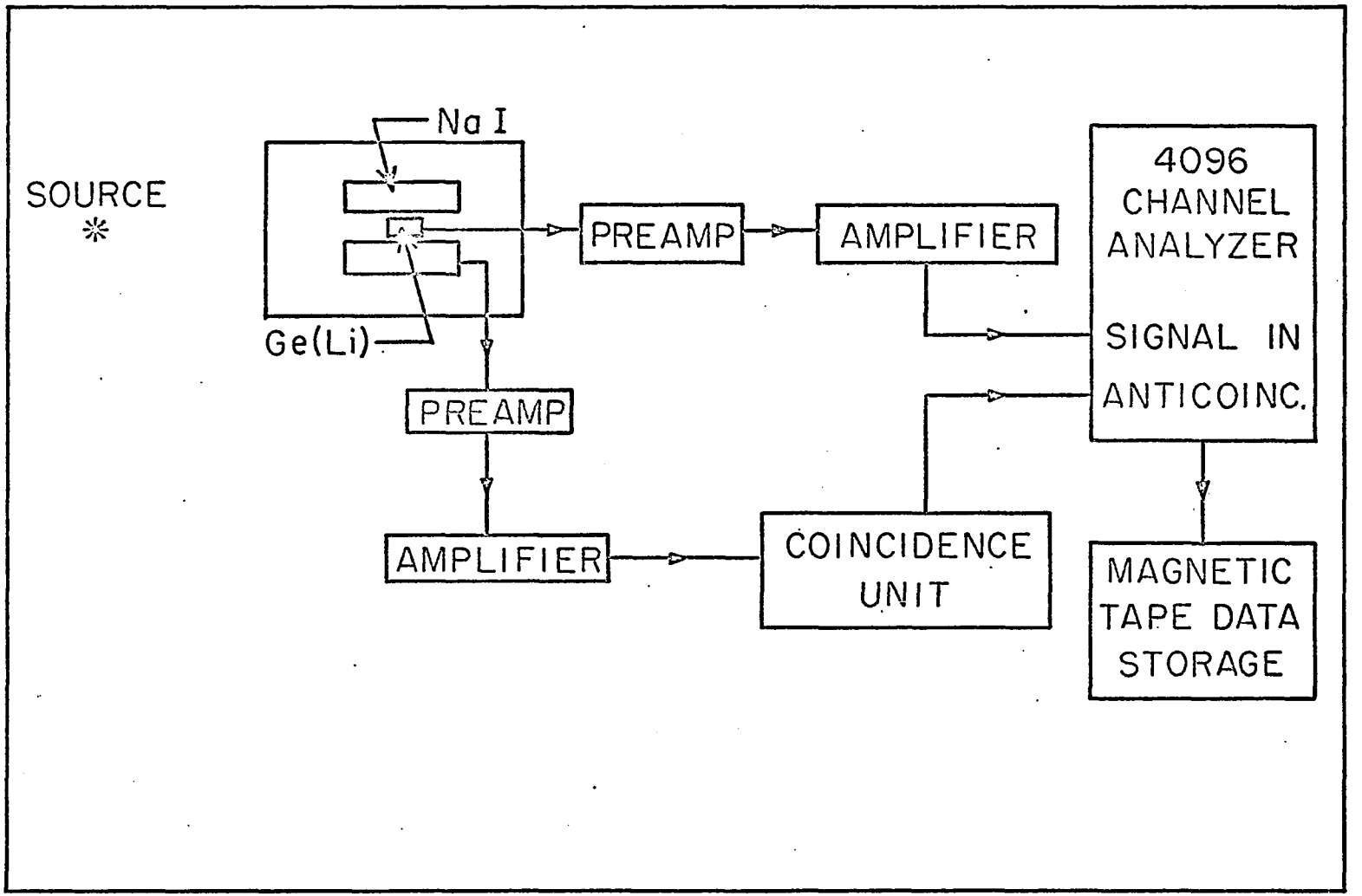

Fig. 6. Instrumentation system for gamma-ray counting.

Autoradiographs were taken of all IAEA sources to obtain an estimate of the distribution of radioactive material in each source. The results indicated that in some cases the radioactive material was distributed over an area larger than that of the ^{235}U samples for which the lead collimator was designed. Therefore, when counting IAEA sources the inner collimator was removed and the detection system not operated in the Compton suppression mode. This insured that all source gamma-rays could see the total front surface of the Ge(Li) detector.

When counting the IAEA sources, Ge(Li) count rates were always less than 200 counts per second and measured analyzer dead times were all less than 0.4%. At least three separate counts of all IAEA sources were made and two counts of the relative sources were taken. For all IAEA sources and for the more intense gamma-rays from the relative sources at least 10^5 counts were obtained in each full-energy peak per counting interval.

CHAPTER 4

DATA ANALYSIS

Ionization chamber data had to be corrected for non-fission events above the thresholds of the discriminators which preceded the scalers and for fission events below the thresholds. Both of these corrections were of the order of one percent and were easily determined by comparing the data from the 200-channel analyzer from counts taken with bare platinum discs in the chamber and with the fission foils in the chamber.

Flux depressions caused by both the platinum backing of the fission foils and the 15 mg ^{235}U samples were not amenable to experimental determinations. The calculations of these flux depressions are described in Appendix A.

The gamma-ray spectra were transferred directly from the multichannel analyzer to magnetic tape after each counting interval. Computer analyses of the gamma spectra were then performed to determine areas of full-energy peaks. These areas were used to calculate the yields from either Equation (2-2, 2-3, or 2-4). A lengthy literature search was performed for all nuclides used in this research to determine best values of half-lives and absolute gamma-ray

intensities to be used in the yield calculations. A tabulation of these data is given in Appendix C.

A weighted least squares curve fit to the efficiency data was also performed. This enabled an accurate interpolation between the point data to obtain the efficiencies at the numerous gamma-ray energies of interest.

Gamma-Ray Spectra Unfolding

Representative gamma-ray spectra taken at 3 hours and 1, 7, and 57 days after irradiation are shown in Appendix B. These four spectra exhibit all of the peaks analyzed in this work.

A least squares fit computer program (Sanders and Holm 1969) performed the full-energy peak integrations on a CDC 6600 computer. The code fits the gamma-ray peaks in an energy region with the function

$$Y(J) = \sum_{I=1}^{N} \left[G(I,J)+EXP1(I,J)+EXP2(I,J) \right] + EXPB(J)$$

where

I indicates the full-energy peak,

J indicates the data point,

N is the number of full-energy lines in the region being fit,

Y(J) is the value of the function,

G(I,J) is the Gaussian,

EXP1(I,J) is the zero-slope exponential tail,

EXP2(I,J) is the exponential tail used to represent the asymmetry of the low-energy side of the Gaussian, and

EXPB(J) is the background contribution.

Figure 7 shows how the function described above fits the 1.6 MeV ^{140}La full-energy peak. This figure was not, however, a result of data taken with the detector used in this experiment and as such the low-energy tail, EXP2, is slightly out of proportion. As shown in Figure 7, this tail is approximately five percent of the Gaussian area while for the detector used in the experiment this tail varied between one-half and one and one-half percent of the Gaussian areas. Two major causes for the asymmetry are known: one is insufficient collection voltage in various regions of the detector; and the other is a combination of counting rate and amplifier response. Due to the baseline restoration on the output of the amplifier and the low counting rates employed in this experiment, this latter effect was negligible. Current Ge(Li) detectors also operate at higher bias voltages than were previously possible, making for more complete charge collection and smaller fractional tail areas.

An example of a fit to data taken in this experiment is shown in Figure 8. The data was taken at 57 days and the

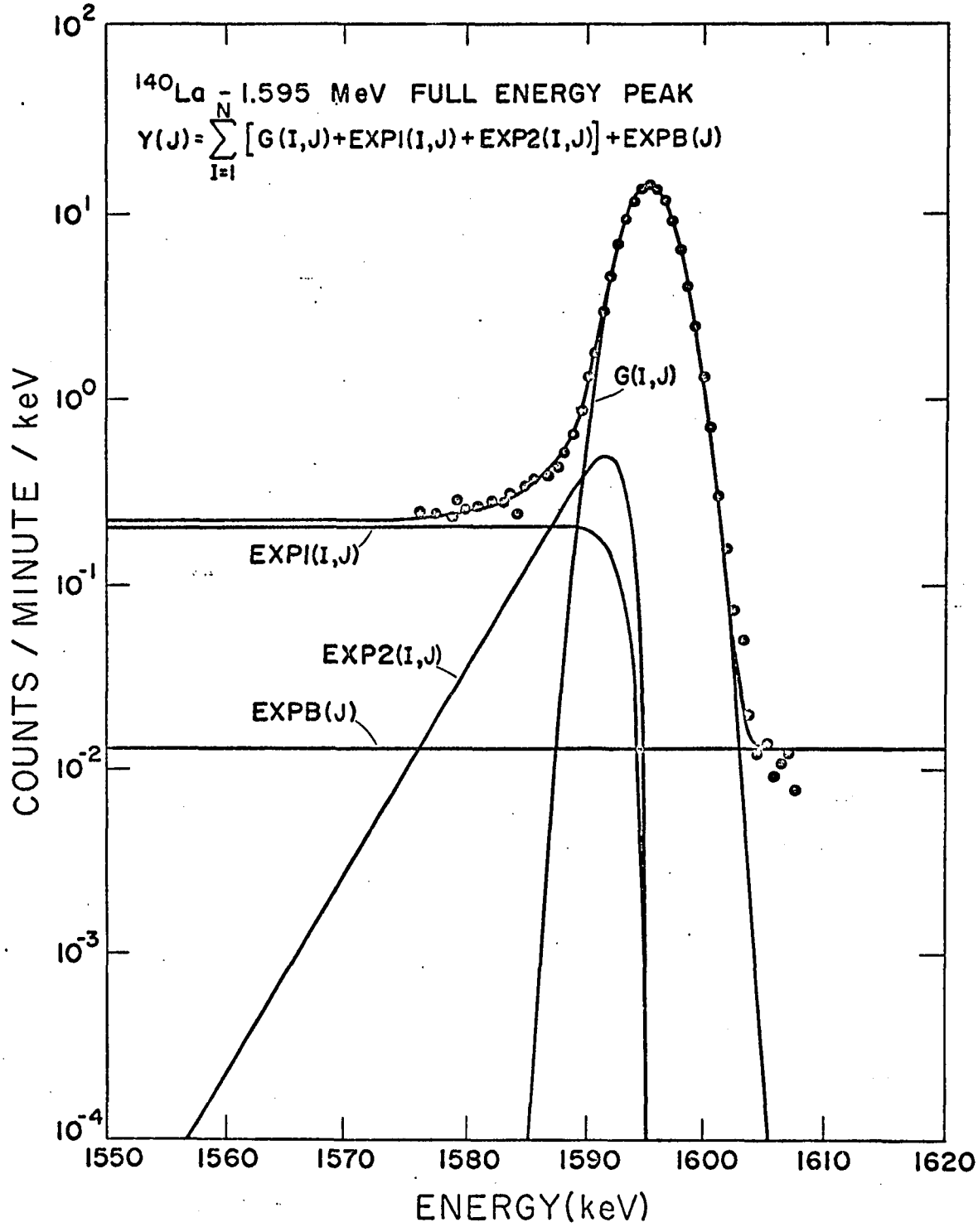

Fig. 7. Example of how the computer code fits a full-energy peak.

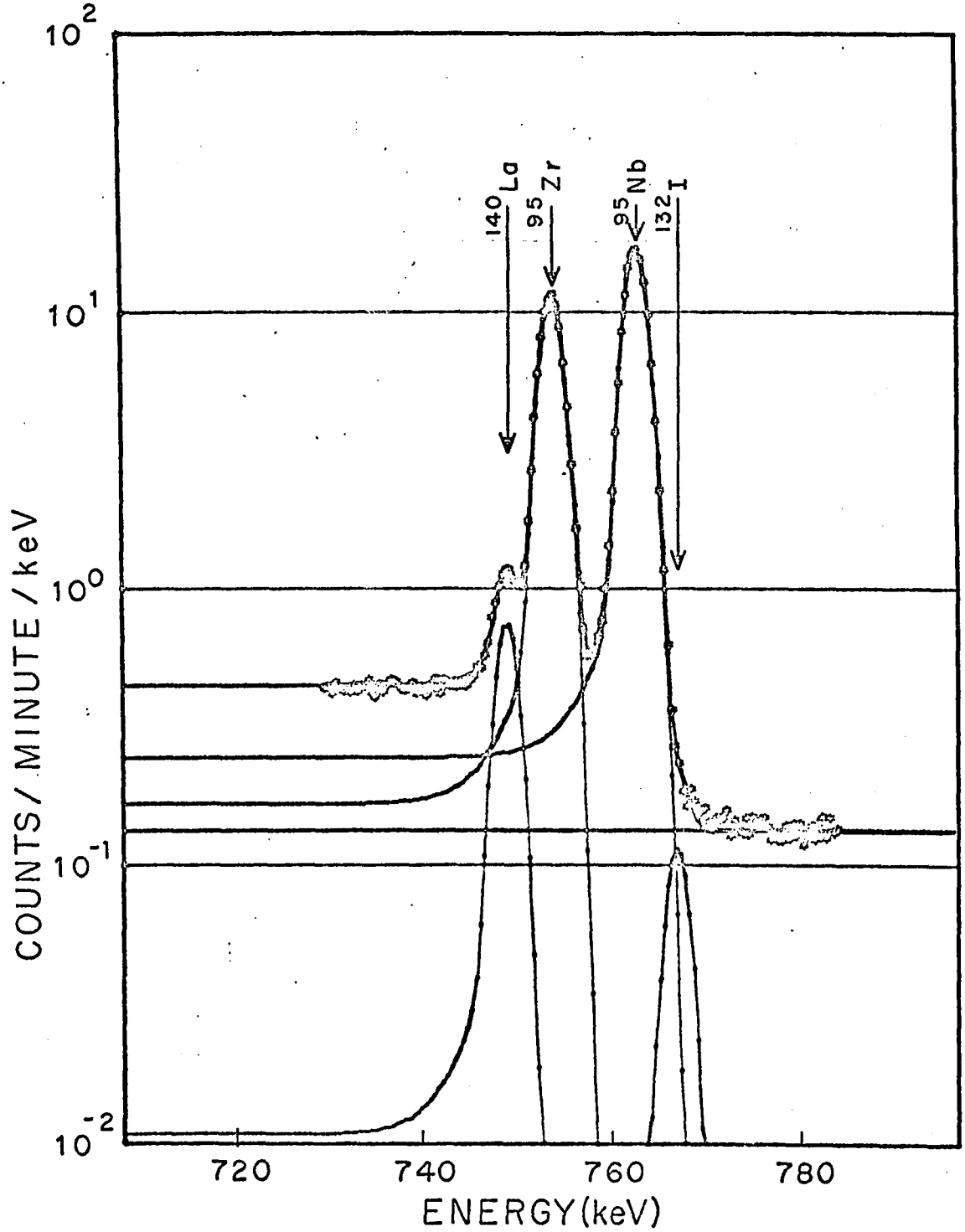

Fig. 8. Example of the fit made to the experimental data.

full-energy peaks fit are from ^{140}La, ^{95}Zr, ^{95}Nb, and ^{132}I. The individual Gaussian and exponential tail areas are not shown for each peak as in Figure 7, instead a smooth curve representing the sum

$$G(I,J) + EXP1(I,J) + EXP2(I,J)$$

is shown for clarity. The computer printout, however, itemizes all parameters, areas, and their deviations calculated in the least squares fit to the data. For consistency and since the asymmetric tail, EXP2, is mainly a result of full-energy events with incomplete charge collection, all full-energy peak areas, including those from the efficiency calibration sources, were taken to be the sum of the Gaussian and exponential tail areas, that is,

$$\text{full-energy peak area} = G(I,J) + EXP2(I,J).$$

Curve-Fitting Ge(Li) Efficiency Data

A weighted least squares spline program was used to interpolate between the efficiency calibration data. This approximation, which is essentially the numerical analogue of the draftsman's spline, consists of fitting the data points with sections of cubics, requiring that the slopes and curvatures be continuous at the junction points. In addition, it is required that the quantity

$$d = \sum_{j=1}^{J} W_j [f(x_j) - y_j]^2 \qquad (4\text{-}1)$$

be a minimum. This is the least squares condition, where W_j is the weight of each data point, y_j the experimental value of the variable, $f(x_j)$ the calculated or spline value of the variable, and J the number of data points.

With this program the user selects both the number of regions to be independently fit by cubics and the boundaries of each region. The efficiency data of this experiment were input in the spline program in three forms:

$$(x_j, y_j) \ , \ (x_j, \ \ell n \ y_j) \ , \text{ and } (\ell n \ x_j, \ \ell n \ y_j)$$

as the data showed varying curvatures in different energy regions when plotted in these forms.

The criterion for goodness of fit over an energy interval used to compare the fits to the three forms of input data was the weighted variance defined as

$$V = \sum_{J=1}^{n} \frac{W_j (f(x_j) - y_j)^2}{n-p} \qquad (4\text{-}2)$$

where the terms in Equation (4-2) are the same as those defined in Equation (4-1) with two exceptions. The weighted variance is defined here not for all data points, J, but

only for those points, n, in a particular energy interval; and p is the number of parameters.

When fitting data of the form (x_j, y_j), the weighting factors were equal to the inverse of the variance of the data points,

$$W_j = \frac{1}{\sigma_{y_j}^2} \quad .$$

With data of the forms $(x_j, \ell n\ y_j)$ and $(\ell n\ x_j, \ell n\ y_j)$, the weighting factors were equal to the inverse of the square of the absolute fractional uncertainties in the efficiency data,

$$W_j = \frac{y_j^2}{\sigma_{y_j}^2} \quad .$$

Yield Calculations

Two short computer codes were written to calculate the cumulative chain yields. One code solved Equations (2-2 and 2-3), and the other solved Equation (2-4).

A few of the fission products studied in this experiment had parents with both non-negligible half-lives and fractional cumulative yields measurably less than unity. In these cases neither Equation (2-3) nor the corresponding form of (2-4) would be appropriate for yield calculations.

For example, consider the yield of ^{138}Cs which has a measured fractional independent yield of 0.047 (Wahl et al. to be published). Thus, the fractional cumulative yield of

^{138}Xe, the parent of ^{138}Cs, is 0.953. Then, for this situation, the total full-energy counts for a particular gamma-ray from ^{138}Cs are the result of a simple decay (e.g., Equation (2-2)) 4.7% of the time and a daughter decaying from a parent (e.g., Equation (2-3)) 95.3% of the time. The form of the yield equation appropriate for this situation is

$$C = 0.047\ (RHS2) + 0.953\ (RHS3), \qquad (4-3)$$

where RHS2 is the right-hand side of Equation (2-2) and RHS3 is the right-hand side of Equation (2-3). If the yield were determined from a relative sample, then forms of Equation (2-4) would replace RHS2 and RHS3 in Equation (4-3). However, the principle is the same for both the standard and relative samples.

For all fission products studied in this work, yields were calculated from gamma-ray spectra taken at two or more times after irradiation for each ^{235}U sample. These yields were averaged for each ^{235}U sample and then further averaged with respect to the different ^{235}U samples.

CHAPTER 5

RESULTS

Cumulative fission product yields were determined for 32 nuclides representing 26 mass chains. Based on the correlation of independent and cumulative yields by Wahl et al. (to be published), only one of the cumulative yields reported herein should be measurably less than the corresponding total chain yield. This fact permitted comparisons between the results obtained from this experiment and studies which used mass spectrometric techniques to determine total chain yields.

Ge(Li) Detector Efficiency

The absolute full-energy peak efficiency of the Ge(Li) detector used in this experiment is shown in Figure 9. The point data shown on the graph are tabulated in Appendix C. Uncertainties in these point data range from about 0.7 to 3.5%.

Uncertainties in the efficiencies for gamma-ray detection studied in this work varied from about 1.0 to 3.0%, depending on the proximity of the energy of the gamma-ray of interest to a calibration point and the computed weighted variance in the energy region.

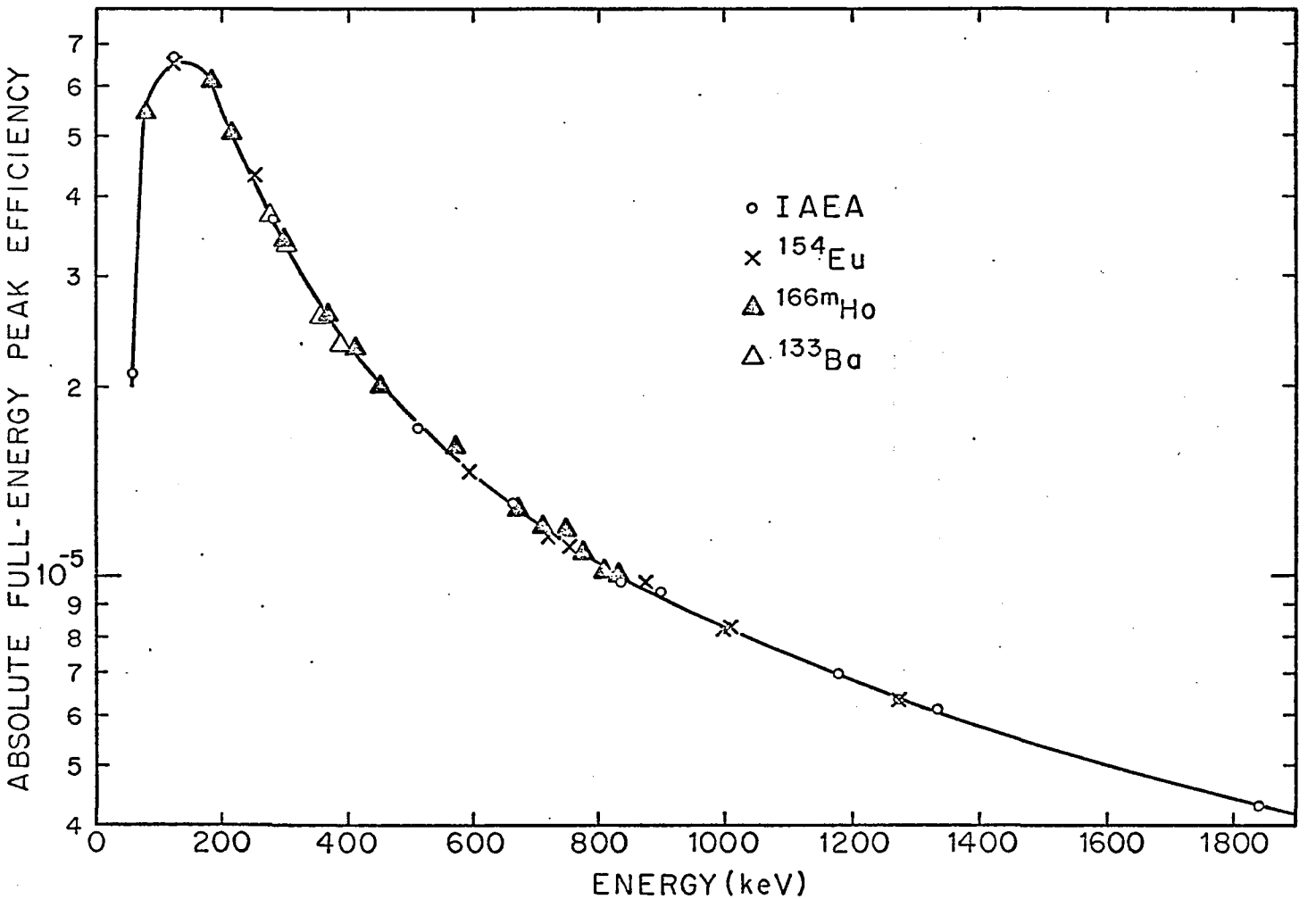

Fig. 9. Ge(Li) detector absolute full-energy peak efficiency.

Fission Product Yields

Cumulative yields determined in this work are given in Table 2 together with values from the two most recent studies on this subject. The results of the study by Lisman et al. (1969) had quoted errors of less than one percent for most of the mass numbers measured. The values from Rider et al. (1967) are a result of a compilation and critical analysis of all research in this field prior to July, 1967. Uncertainties were suggested as two percent or greater based on the data available at that time.

A notable omission from the results of the 1969 study is a yield for mass 135. The long irradiation time and large cross section of ^{135}Xe caused burnup uncertainties and prevented an accurate yield determination. Therefore, for this important mass chain, the gamma-ray spectroscopy technique offers a significant improvement over other experimental methods.

Error Estimations

The individual parameters in Equations (2-2, 2-3, and 2-4) from which the yields were calculated will now be discussed with respect to their uncertainties.

Typically the errors in determining full-energy peak areas were in the range $0.2 \leq \Delta C \leq 1.0\%$ for high-intensity transitions. Larger errors were associated with only those peaks from nuclei with half-lives less than a few hours or

Table 2. Percent chain yields in the thermal fission of ^{235}U.

FISSION PRODUCT	THIS WORK	MASS NO.	LISMAN	RIDER
^{85m}Kr	1.36 ± 0.05	85	1.30	1.30
^{87}Kr	2.29 ± 0.18	87	2.54	2.50
^{88}Kr	3.73 ± 0.22	88	3.61	3.58
^{91}Sr	5.31 ± 0.47	91	5.90	5.90
^{91m}Y	5.77 ± 0.24			
^{92}Sr	6.00 ± 0.17	92	5.95	6.03
^{93}Y	6.82 ± 0.62	93	6.34	6.48
^{95}Zr	6.40 ± 0.16	95	6.45	6.41
^{95}Nb	6.34 ± 0.16			
^{97}Zr	6.17 ± 0.11	97	5.86	6.21
^{97}Nb	6.15 ± 0.11			
^{99m}Tc	6.14 ± 0.17	99	6.14	6.19
^{103}Ru	3.22 ± 0.09	103		3.0
^{106}Rh	0.401±0.019	106	0.389	0.39
^{131}I	2.68 ± 0.07	131	2.79	2.91
^{132}Te	4.17 ± 0.10	132	4.16	4.33
^{132}I	4.38 ± 0.12			
^{133}I	6.59 ± 0.19	133	6.73	6.67
^{133}Xe	6.67 ± 0.52			
^{134}I	7.60 ± 0.15	134	7.51	7.92
^{135}I	6.31 ± 0.51	135		6.43
$^{135}Xe^{a}$	6.71 ± 0.18			
^{137}Cs	6.20 ± 0.18	137	6.28	6.18

Table 2, Continued.

FISSION PRODUCT	THIS WORK	MASS NO.	LISMAN	RIDER
^{138}Cs	6.91 ± 0.32	138	6.80	6.60
^{139}Ba	6.31 ± 0.27	139		6.28
^{140}La	6.40 ± 0.11	140	6.31	6.30
^{141}Ce	5.76 ± 0.17	141	5.50	5.81
^{142}La	5.70 ± 0.21	142	5.88	5.84
^{143}Ce	5.76 ± 0.48	143	5.90	5.87
^{144}Ce	5.79 ± 0.43	144	5.42	5.34
^{147}Nd	2.29 ± 0.09	147	2.12	2.25
^{149}Nd	1.08 ± 0.06	149	1.00	1.09

a. Fractional independent yield of ^{135}Xe taken as 0.04 ± 0.01 from Wahl et al. (to be published).

greater than one year. In these instances either the overlap of peaks or a low value of the peak to background ratio prevented accurate integration.

Calculating the number of fissions during each standard sample irradiation was accurate to about 1.1%. This was due mainly to uncertainties in the fission foil masses (≅ 1.0%) and flux depression corrections (≅ 0.4%).

Above 250 keV the estimated precision of the efficiency determinations was always less than 2.0% and for some energy ranges less than 1.5%. For example, due to the number of high accuracy IAEA calibration points between 800 and 1400 keV and the small weighted deviation from the computer fit to the data, absolute efficiencies are believed to about 1.0% in this energy range. Below 250 keV errors were estimated to be between 1.5 and 3.0%.

Whenever a yield value from this work has an error greater than about 2.5%, it is due largely to uncertainties in the absolute gamma-ray intensity. With the current widespread use of high resolution Ge(Li) detectors much work has been done in the past few years on improving gamma-ray intensity data and decay scheme data in general. However, after a thorough literature search it is apparent that large variations in the data still exist in many cases. As newer and more accurate decay scheme data become available the yields reported herein may be updated; the gamma-ray

intensities used in the yield calculations and their uncertainties are tabulated in Appendix C.

Listed also in this table are the half-lives used in this experiment. These are almost entirely 1.0% or better values. As such, half-life uncertainties contributed only a small fraction to the total uncertainties.

The three remaining factors, f_{SA}, T_L, and the times t_1, t_2, and t_3, all contributed negligibly to the total yield errors. The self-absorption factor, f_{SA}, was calculated for a 48.0 mg/cm^2 uranium disc using the self-absorption equation for a thin sheet,

$$f_{SA} = \frac{1}{\mu d}\left(1-e^{-\mu d}\right),$$

where μ is the total attenuation coefficient and d is the material thickness. Values of μ were obtained from a compilation by Storm and Israel (1967). The point values were plotted and values of f_{SA} at the energies of interest were determined visually from Figure 10.

Analyzer dead times when counting the standard samples were always less than 3.0%. Due to the small values of the dead times and the accuracy with which they were measured, uncertainties in the system live time, T_L, were always less than 0.1%.

The absolute value of t_1, the irradiation time, was recorded to an accuracy of ± 10 seconds. However, the

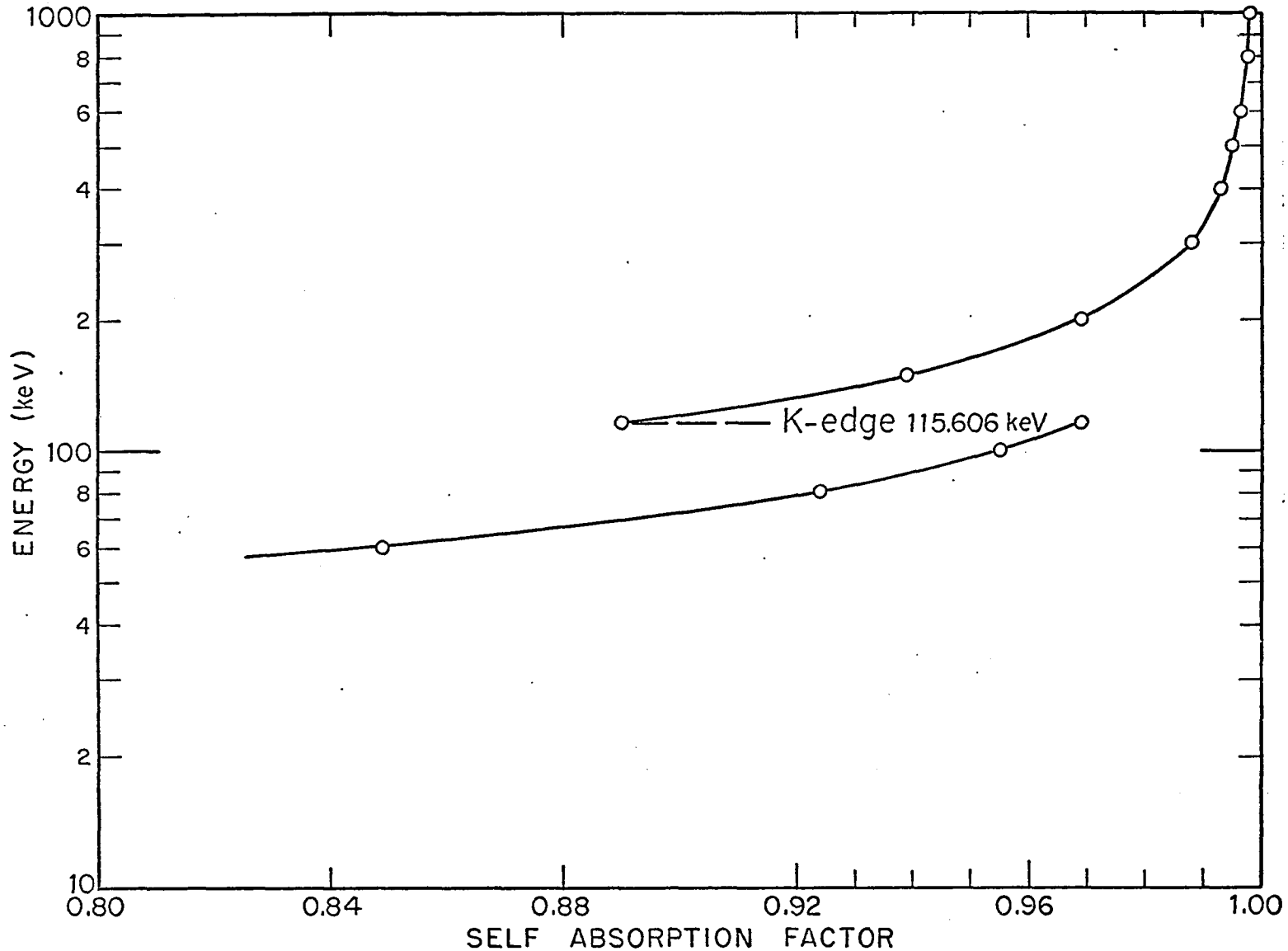

Fig. 10. Gamma-ray self-absorption for 15 mg ^{235}U samples.

counting interval, $t_3 - t_2$, was always measured to an accuracy of better than $\pm$ 0.5 seconds. Thus, there are essentially no errors due to uncertainties in the recorded times.

CHAPTER 6

CONCLUSIONS

Determining fission product yields using gamma-ray spectroscopy has the obvious advantages of speed and convenience over other techniques for fission yield studies. Although the errors quoted for the results of this experiment are greater than for most of the recent mass spectrometric data, an important exception is mass number 135. For the short irradiation times used in this experiment ^{135}Xe burnup was negligible and an accurate yield was obtained. With the aid of more accurate decay scheme data all of the yields determined in this experiment could be stated with uncertainties of less than 3.0%.

As high isotopic purity fission foils with deposits of ^{235}U or ^{239}Pu are in existence at Los Alamos Scientific Laboratory and possibly other places, studies similar to this one for fast neutron irradiations of ^{235}U and for both fast and thermal irradiations of ^{239}Pu would be very worthwhile. Also there exists the possibility of calibrating foils of other fissile or fertile materials, for example ^{241}Pu, by absolute alpha counting and then performing research of this type.

Further research in this field could also include sample irradiations followed promptly by dissolution and chemical separation of the fission fragments. This would greatly simplify the individual gamma spectra and enable determinations of independent yields of many isotopes.

APPENDIX A

FLUX DEPRESSION CALCULATIONS

Both during the calibration of the fission foils used in this experiment and during the standard sample irradiations, flux differences due to neutron absorption existed between the two samples of ^{235}U in the ionization chamber. When calibrating the fission foils the platinum disc depressed the flux slightly, and for the standard sample irradiations the 15 mg ^{235}U samples caused significant flux depressions.

Based on recent neutron spectra measurements from a fission source in graphite (Profio, Antunez and Huffman 1969) and knowledge of the ionization chamber-reactor core distance in the graphite thermal column of the Water Boiler Reactor, it was assumed that the thermal flux would very closely approximate a 2200 m/sec Maxwellian distribution. The irradiation conditions in the fission chamber approximated the irradiation of a purely absorbing sample in a void. This statement follows from the facts that the sample size was much less than the dimensions of the chamber, and there was no appreciable scattering material within a few cm of the sample.

Theory

The depression of thermal neutron fluxes and densities by absorbing foils has been the subject of several papers (Dalton and Osborn 1961; Hanna 1961, 1963). In these papers the major emphasis has been on calculating the average monoenergetic flux in a sample. The flux shapes through absorbing samples and outside of them have been of lesser interest and very little published material appears on these subjects.

A 1/v absorber in a Maxwellian flux actually responds to the neutron density which due to spectral hardening is depressed slightly more than the flux. For monoenergetic calculations these quantities are the same. It will be shown later that the depressed neutron flux and density are very similar for the experimental conditions of this research.

If a sample is irradiated in a cavity so large that a vanishingly small number of neutrons which pass through the sample are ever scattered back through the sample again, the incident flux is not perturbed by the sample and the only effect is that of self-shielding. Then, for a monoenergetic, isotropic flux and a purely absorbing disc-shaped sample, the ratio of the average flux in the sample to the unperturbed flux is

$$\bar{\phi}/\phi_0 = \frac{\alpha}{2b}(1+\epsilon) \qquad \text{(A-1)}$$

where b is the sample thickness in mean free paths, $\alpha = 1-2E_3(b)$, and ϵ is the edge effect correction given by Hanna (1963).

For a sample with an infinite radius and a nonzero (isotropic) scattering cross-section, Hanna (1963) gives for the flux ratio,

$$\bar{\phi}/\phi_o = \frac{\alpha(b)}{2b} + \frac{b_s}{2b} K(b). \qquad \text{(A-2)}$$

In this equation b_s and b are calculated from the scattering and total mean free paths respectively, and K(b) is given by

$$K(b) = 4.81b - 28.4b^2 + 74.7b^3$$

to within a few percent for b less than 0.15. Equation (A-2) also only applies to the case of a monoenergetic, isotropic flux and irradiation in a large cavity.

The analogues to Equation (A-1) for a 1/v absorber in a Maxwellian neutron spectrum are given by Hanna (1963) as convergent series for both neutron flux and density depressions. It has also been pointed out by Hanna(1961) that in using Equation (A-1) or (A-2) to calculate the response of a thin disc sample to a Maxwellian flux, the appropriate cross-section value is

$$\Sigma = (2/\pi^{\frac{1}{2}})\,\Sigma_o$$

where Σ_o is the cross-section at the modal velocity.

A literature search revealed no equations similar to those described above for the flux or neutron density outside of an absorbing sample.

A straightforward derivation for the isotropic, monoenergetic flux as a function of distance normal to a purely absorbing disc and along the center-line of the disc resulted in the equation

$$\phi(r=o,\ z) = \frac{\phi_o}{2}\ 1 + \cos\theta'\left[1-E_2\ \frac{b}{\cos\theta'}\ \right]+ E_2(b) \qquad \text{(A-3)}$$

where $\cos\theta' = z/[R^2+z^2]^{\frac{1}{2}}$ and R is the radius of the disc. This derivation also assumed a negligible physical thickness as edge effects were neglected. Evaluation of Equation A-3 at z = 0.0 is then the flux at the surface of the absorbing disc. An attempted derivation for points off the axis of the disc resulted in non-integrable functions.

An accurate calculation of the average flux in a non-flux depressing sample, in the presence of an absorbing sample, could be made with Equation A-3 if two conditions were fulfilled. First the radial variation of the flux in both samples would have to be the same; and second, the flux in the absorbing sample would have to be flat in the axial direction. As neither of these conditions would be accurate approximations to the actual situation of irradiating the standard samples in the presence of fission foils, a computer analysis of the problem was performed.

Computer Method of Calculating Flux Depressions

The validity of using the method of analysis described later in this section was determined from two considerations: the experimental configuration of the samples in the ionization chamber and comparisons and analyses of results from Equations A-1, A-2, A-3, and those for a 1/v absorber in a Maxwellian flux (Hanna 1963).

There was no appreciable scattering material within a few cm of the fission foil and standard sample when in the ionization chamber. Thus, to the extent that neutrons passing through the ^{235}U samples had a negligible probability of being scattered back through them, the flux and neutron density depression equations described previously are valid. Using these equations, calculations were made for the 15 mg ^{235}U samples used in this experiment.

The monoenergetic flux depressions calculated from Equation (A-1), absorption only, and Equation (A-2), absorption and scattering, differed by less than 0.1% indicating that scattering in the sample was negligible. Neutron density depressions were calculated from the convergent series given by Hanna (1963) for a 1/v absorber in a Maxwellian flux and Equation (A-1) using the modified cross section described previously. Results of this latter comparison differed by approximately 0.5%, thus it was decided to use a monoenergetic calculation in the computer

analysis. A general-purpose point-kernel program, QAD (Malenfant 1967), was used to calculate the neutron density depressions where Equations A-1 and A-3 were not applicable. The neutron absorption problem was treated as a simple one energy group exponential attenuation problem without scattering.

To mock-up an isotropic flux of neutrons in the fission chamber, 1600 isotropic point sources were distributed over the surface of a sphere surrounding the fission foil and ^{235}U sample. In all calculations the point at which the flux was calculated was at the center of the spherical shell source. To calculate the flux depression at various points in the ^{235}U sample and in the fissile deposit the shell source was moved relative to the samples. In this way the flux was always calculated at the center of the source distribution. This seemingly cumbersome procedure was made necessary by the fact that the flux inside a spherical shell source in a vacuum emitting neutrons isotropically is not a constant, but a function of radial position (Case, de Hoffmann, and Placzek 1953). The number of source points was determined by observing the flux convergence as the number of source points was increased.

As slight differences existed between the materials constituting the fissions foils used in this experiment and the J-11 reference foils, a flux depression calculation was

also performed for the fission foil calibration geometry.

Results

For comparison purposes and to insure that the QAD source point distribution was sufficient, a computer analysis of the flux depression in a bare 15 mg ^{235}U sample was performed and compared to the value calculated from Equation (A-1). The results differed by about 0.2%. Thus, for obtaining flux values to be used in a ratio it was decided that QAD calculations would be sufficiently accurate.

Average relative flux values in the fissile deposit and in the 15 mg ^{235}U sample were calculated for the standard sample irradiation geometry. The QAD results are 0.897 and 0.861 respectively relative to an unperturbed flux value of 1.0.

During fission foil calibrations there were slight flux differences in the two fissile deposits. Computer results are 0.9815 and 0.9880 for the fissile deposits on platinum prepared for this work and the J-11 calibration foils respectively.

APPENDIX B

FISSION PRODUCT SPECTRA

Gross fission product spectra taken during the course of this research are presented on the following pages. Spectra taken at 3 hours and 1, 7, and 57 days after irradiation and for gamma-ray energies between 80 and 1600 keV are shown. Although numerous other spectra were taken at different times after irradiation, these exhibit all of the peaks analyzed.

No attempt was made to determine gamma-ray energies; those shown in the figures are current literature values. For identification of the unlabeled peaks in these spectra consult the work of Murri and Heath (1968). The reason that some prominent peaks are unlabeled, indicating that they were not used in the data analysis, is that they arise from less intense and therefore, in general, less accurately known transitions in a nuclide which is characterized by a more intense gamma-ray which is labeled.

Fig. 11. Gross fission product gamma-ray spectrum from the thermal fission of ^{235}U, taken at 3 hours after irradiation.

The irradiation time was 1 minute and the 4096 channel data is presented in six frames. The energy range of the data is approximately 40 to 1600 keV.

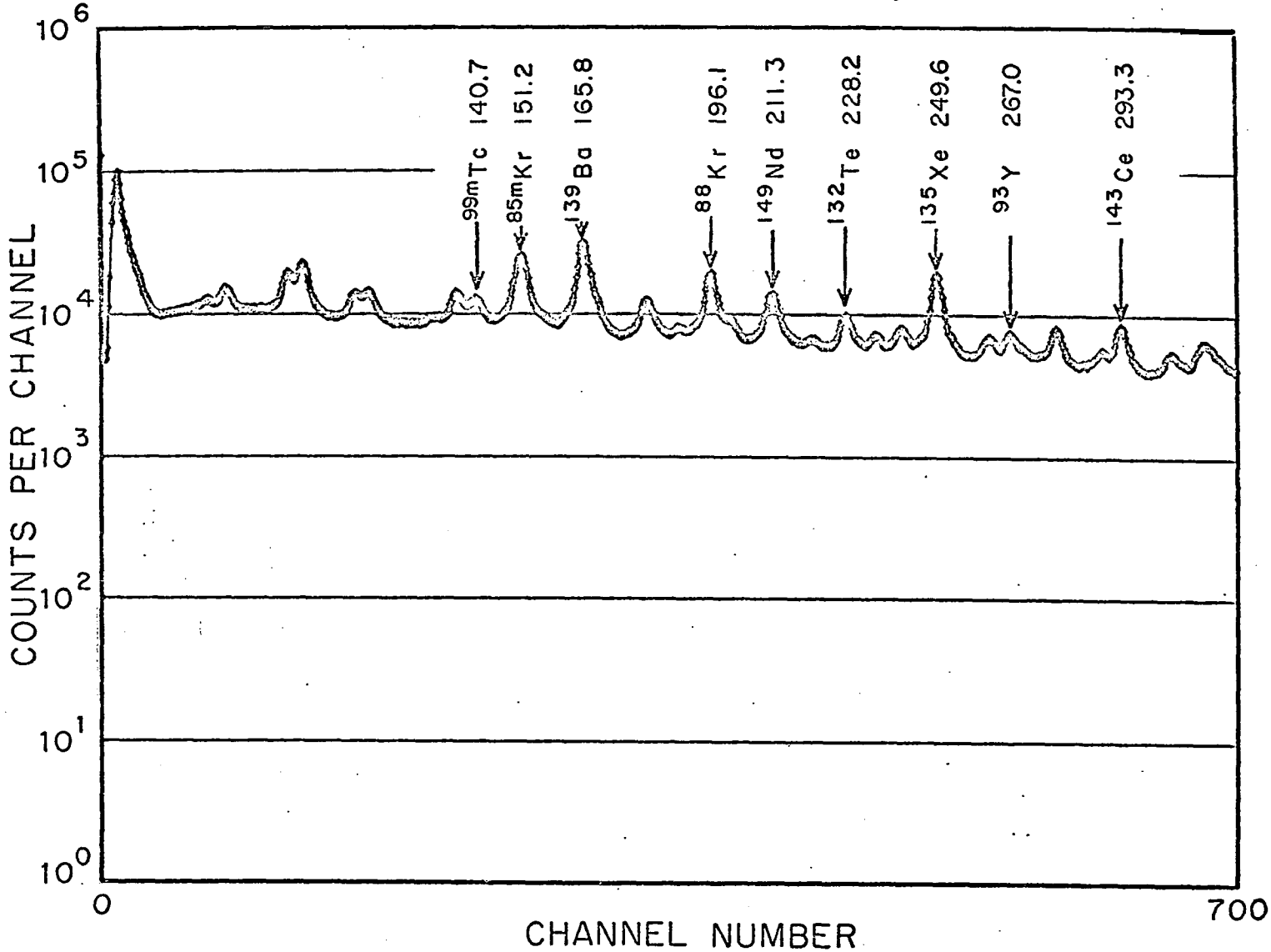

Fig. 11. ^{235}U gamma-ray spectrum at 3 hours after irradiation.

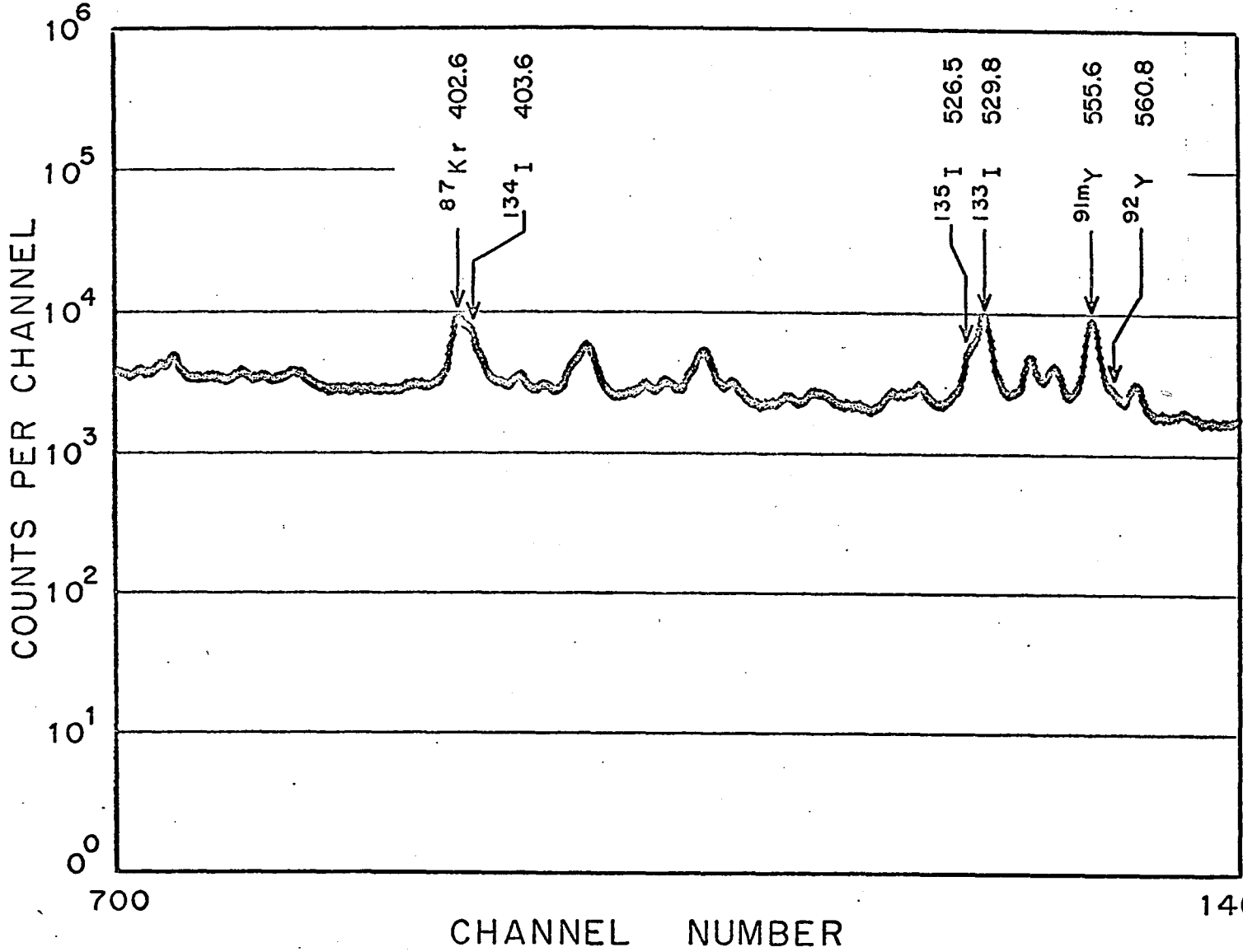

Fig. 11. ^{235}U gamma-ray spectrum at 3 hours after irradiation, Continued.

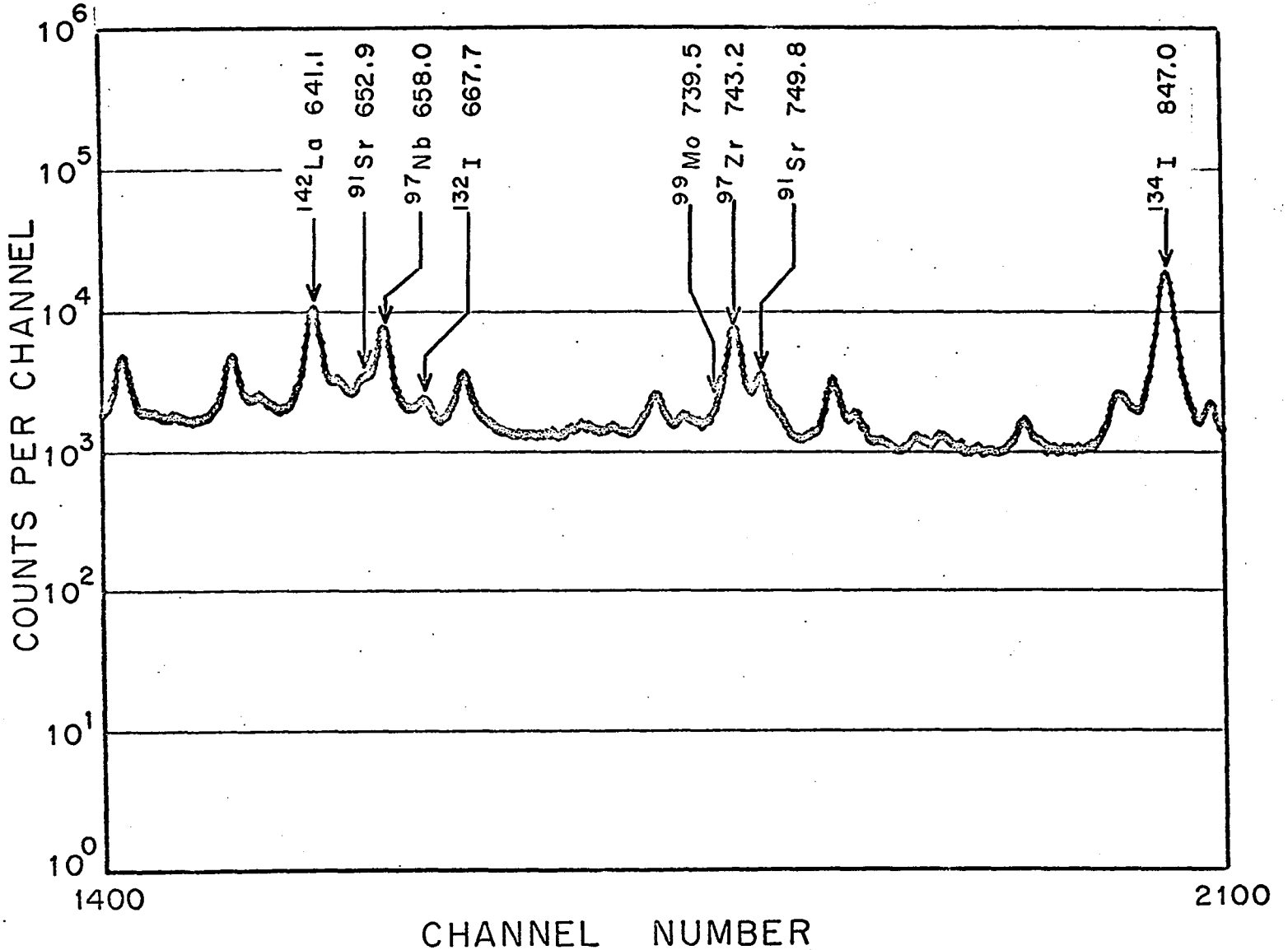

Fig. 11. ^{235}U gamma-ray spectrum at 3 hours after irradiation, Continued.

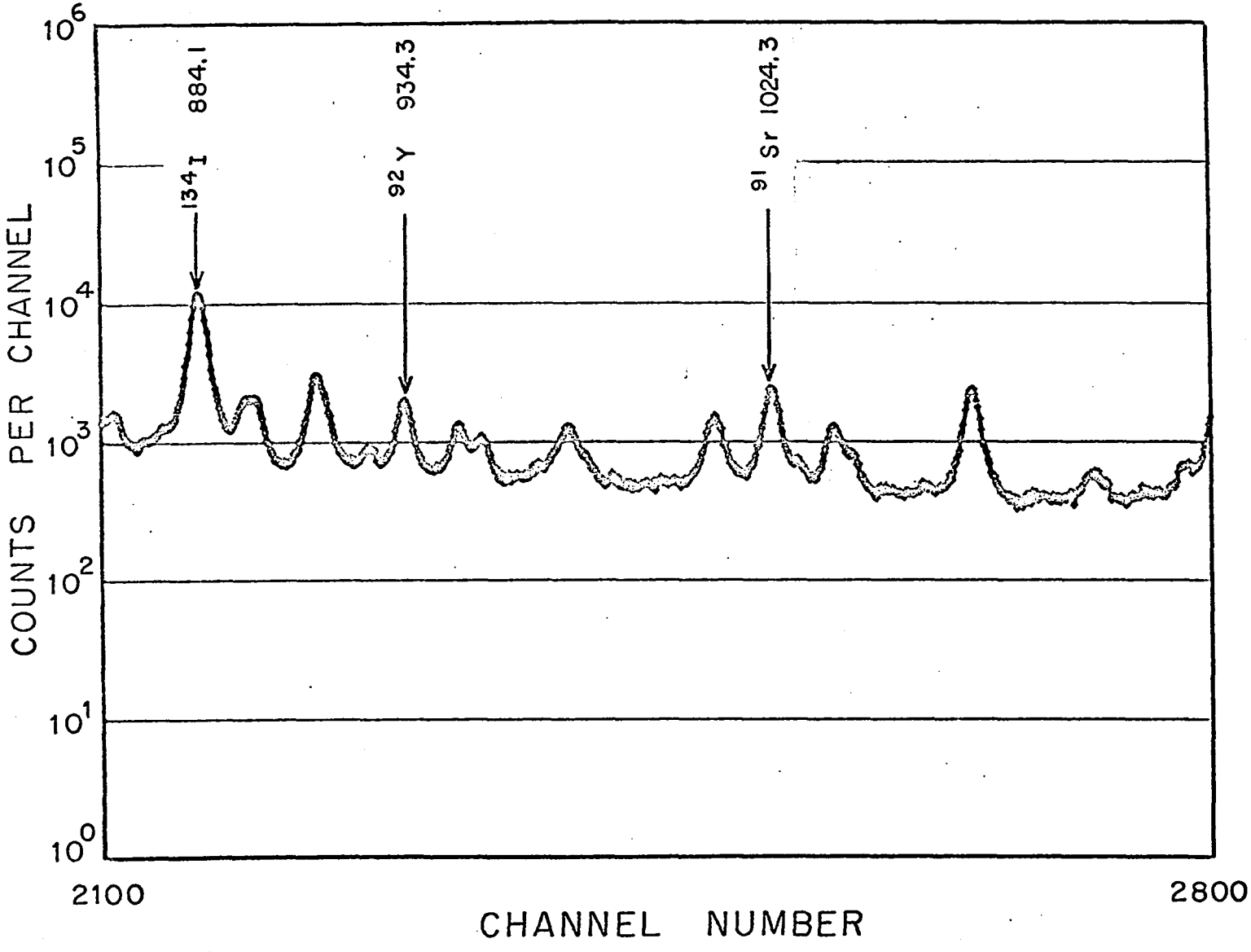

Fig. 11. ^{235}U gamma-ray spectrum at 3 hours after irradiation, Continued.

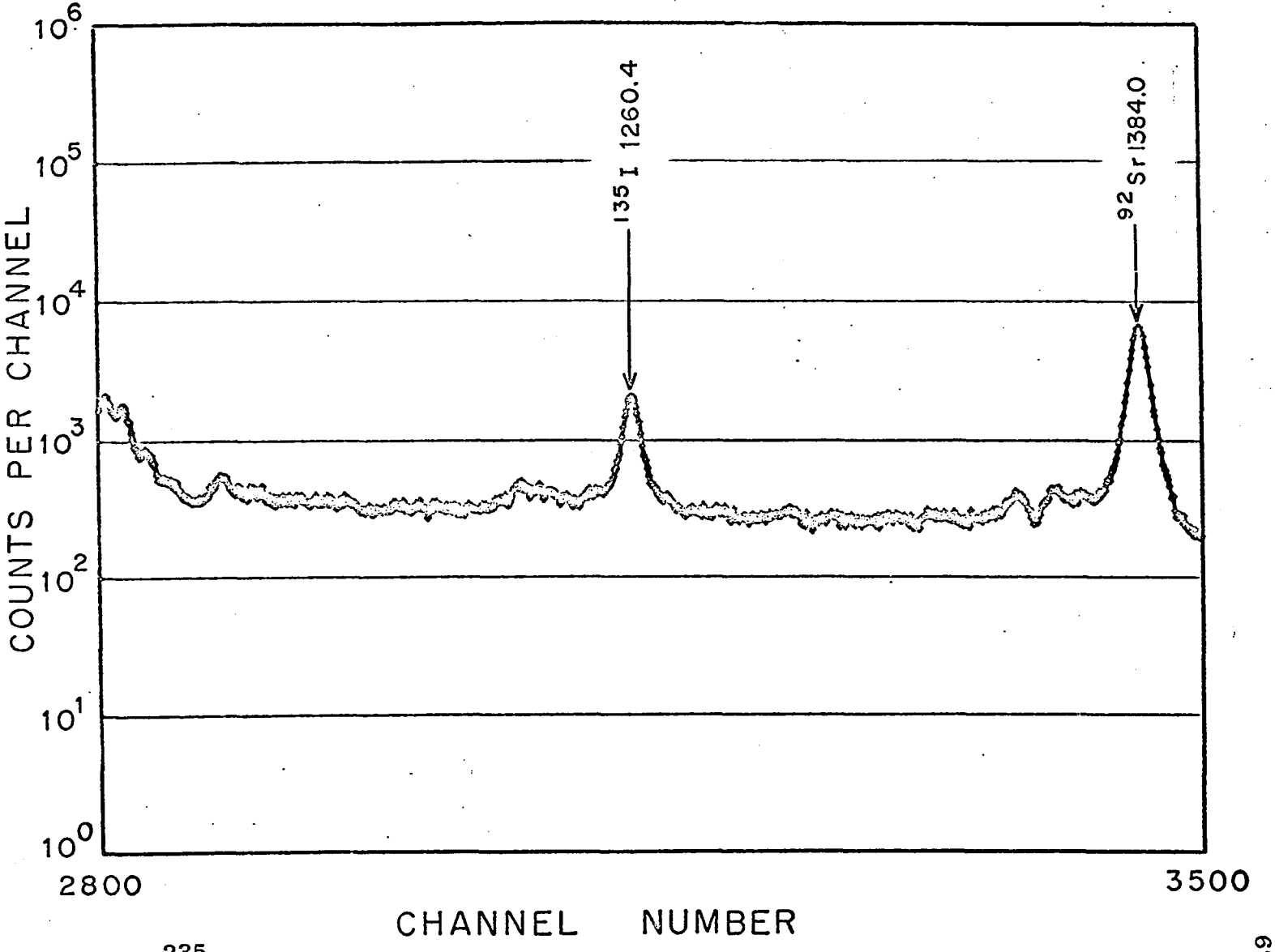

Fig. 11. ^{235}U gamma-ray spectrum at 3 hours after irradiation, Continued.

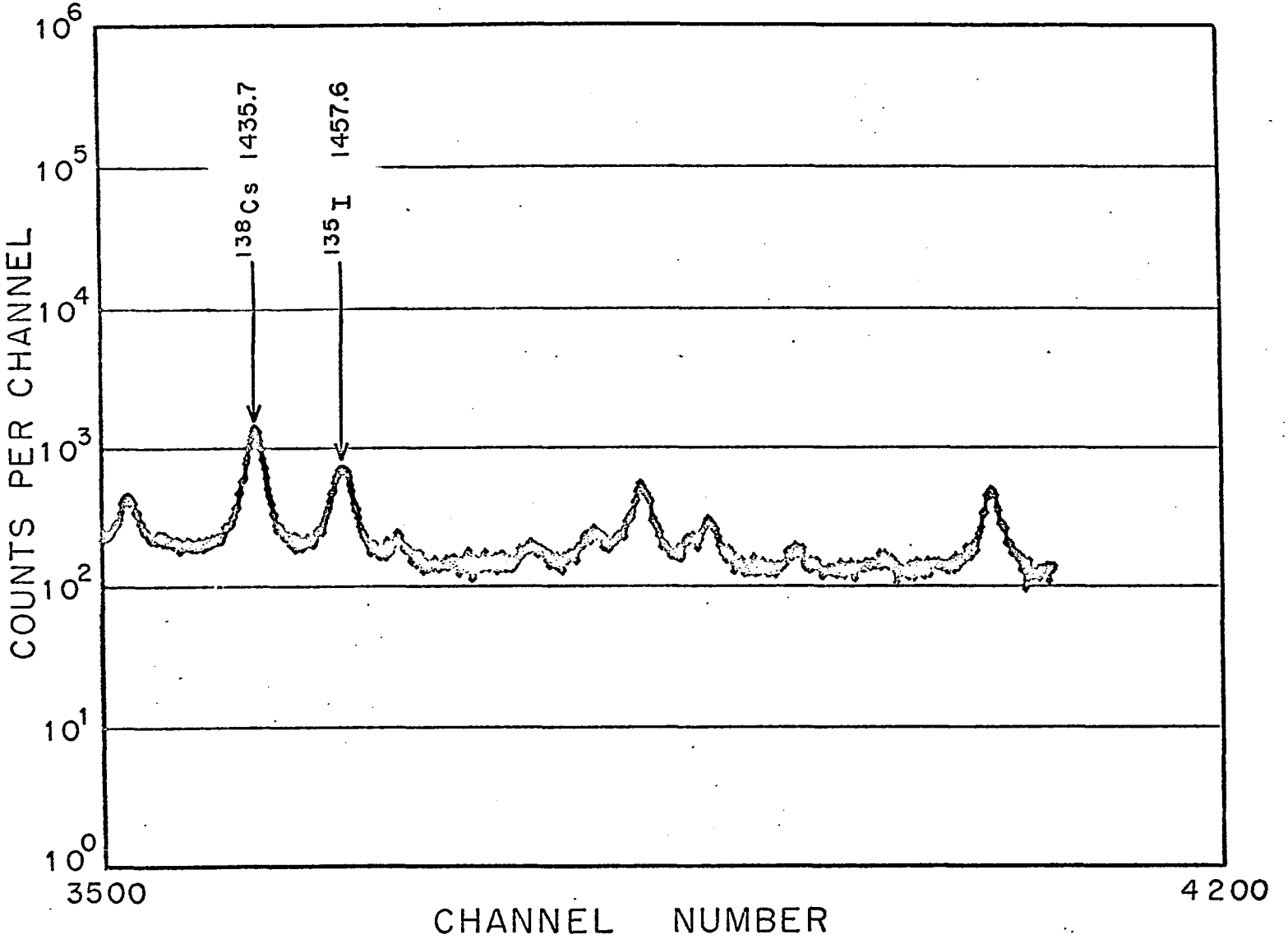

Fig. 11. ^{235}U gamma-ray spectrum at 3 hours after irradiation, Continued.

Fig. 12. Gross fission product gamma-ray spectrum from the thermal fission of ^{235}U, taken at 1 day after irradiation.

The irradiation time was 1 minute and the 4096 channel data is presented in six frames. The energy range of the data is approximately 40 to 1600 keV.

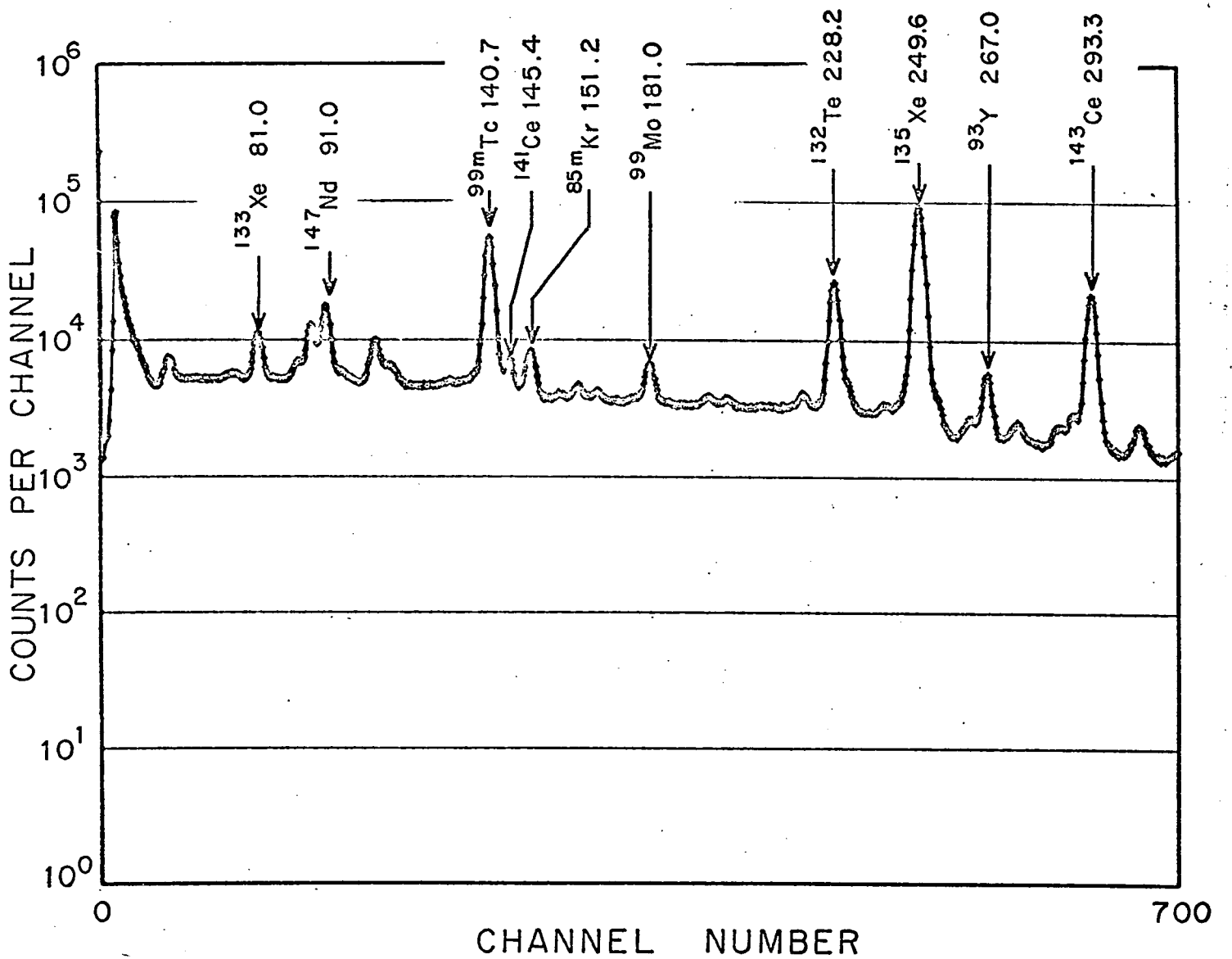

Fig. 12. ^{235}U gamma-ray spectrum at 1 day after irradiation.

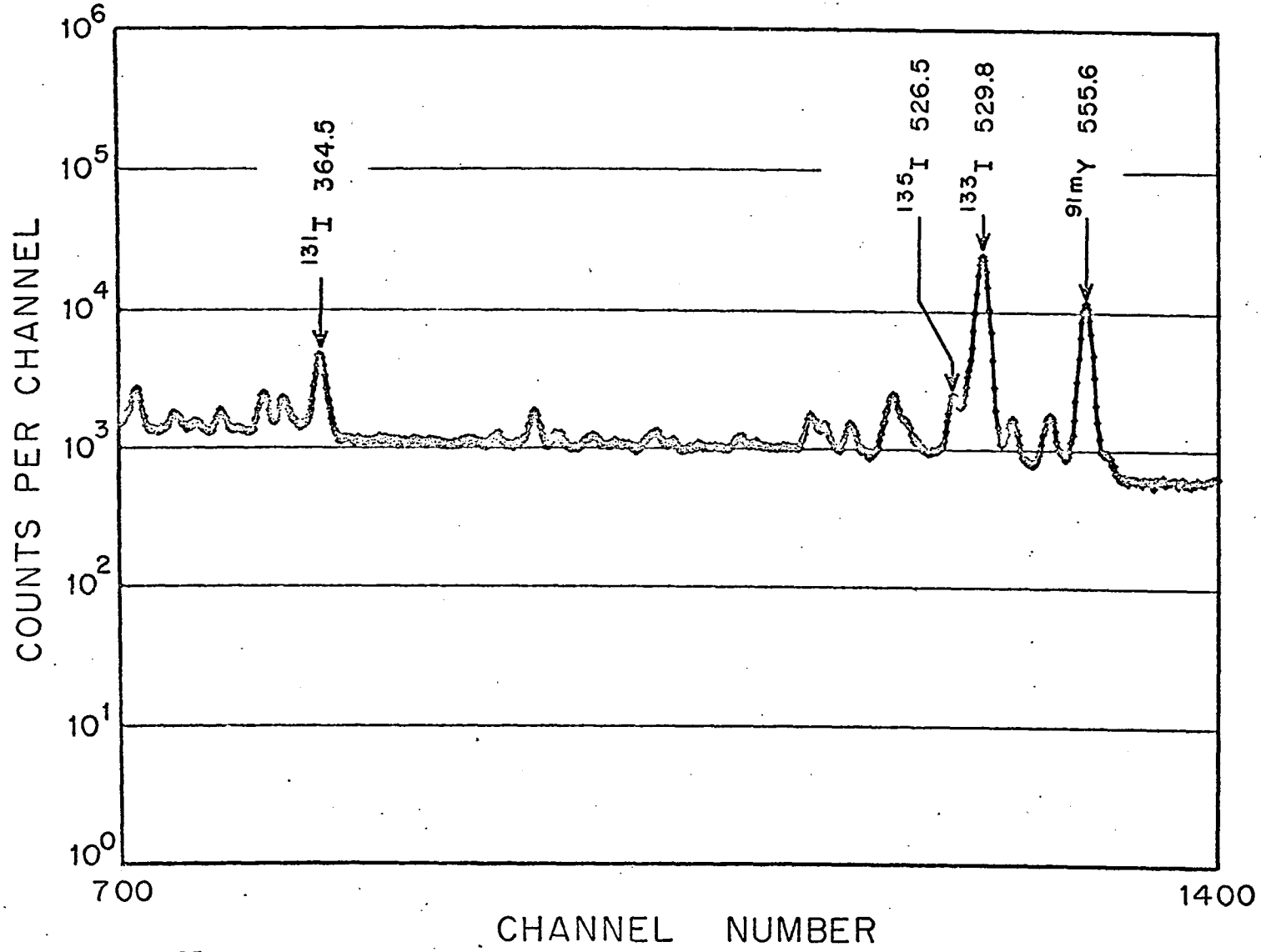

Fig. 12. ^{235}U gamma-ray spectrum at 1 day after irradiation, Continued.

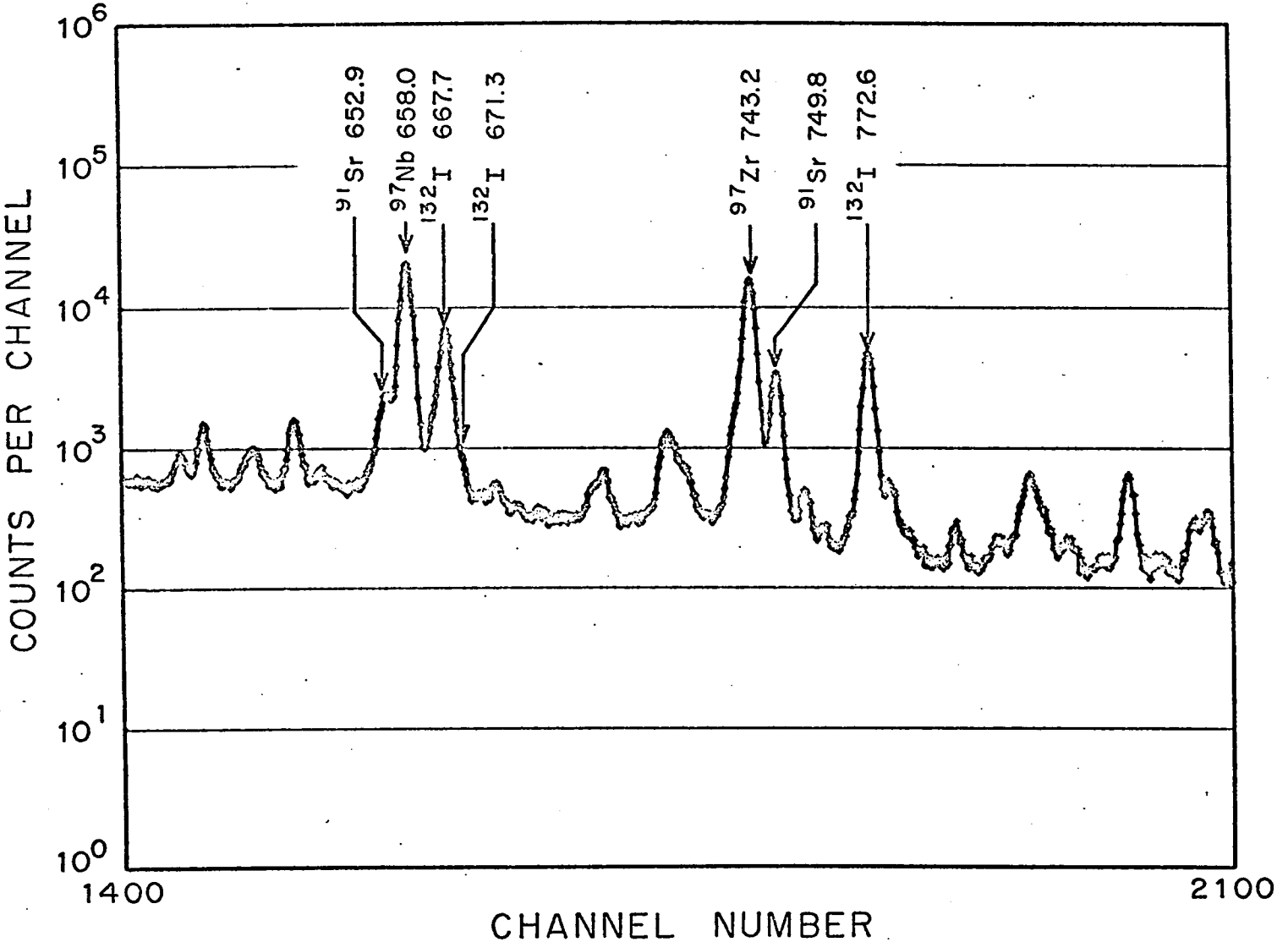

Fig. 12. ^{235}U gamma-ray spectrum at 1 day after irradiation, Continued.

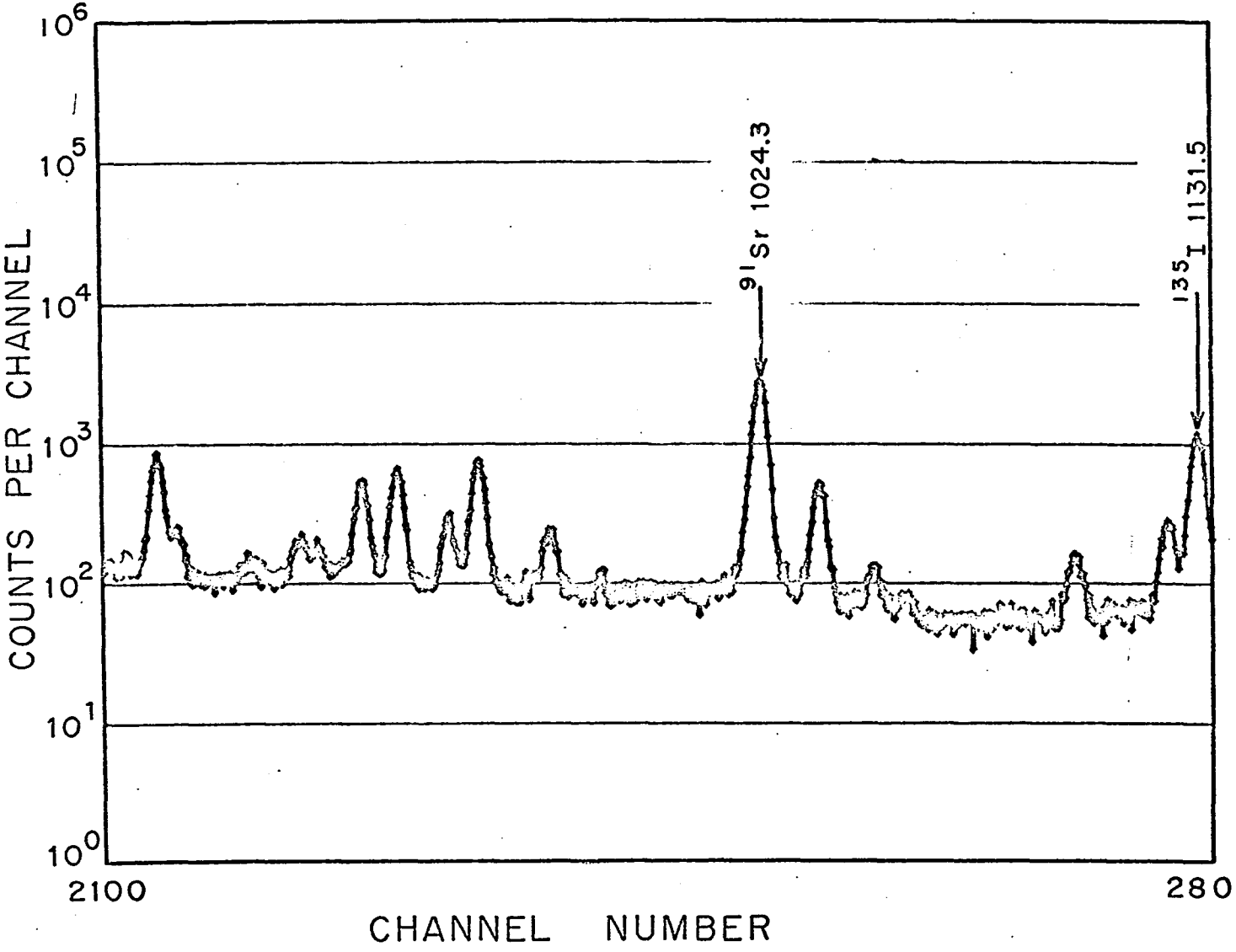

Fig. 12. ^{235}U gamma-ray spectrum at 1 day after irradiation, Continued.

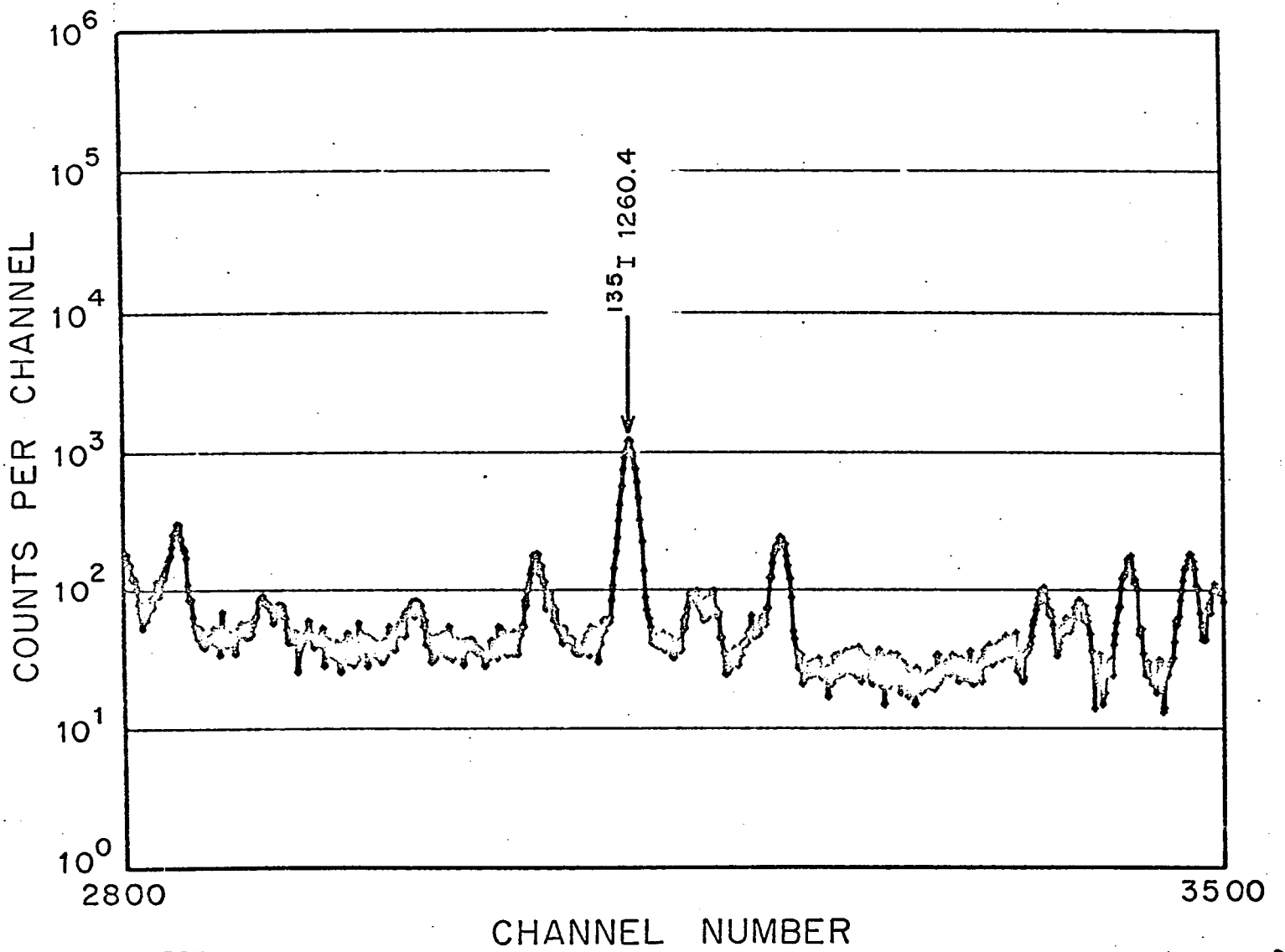

Fig. 12. ^{235}U gamma-ray spectrum at 1 day after irradiation, Continued.

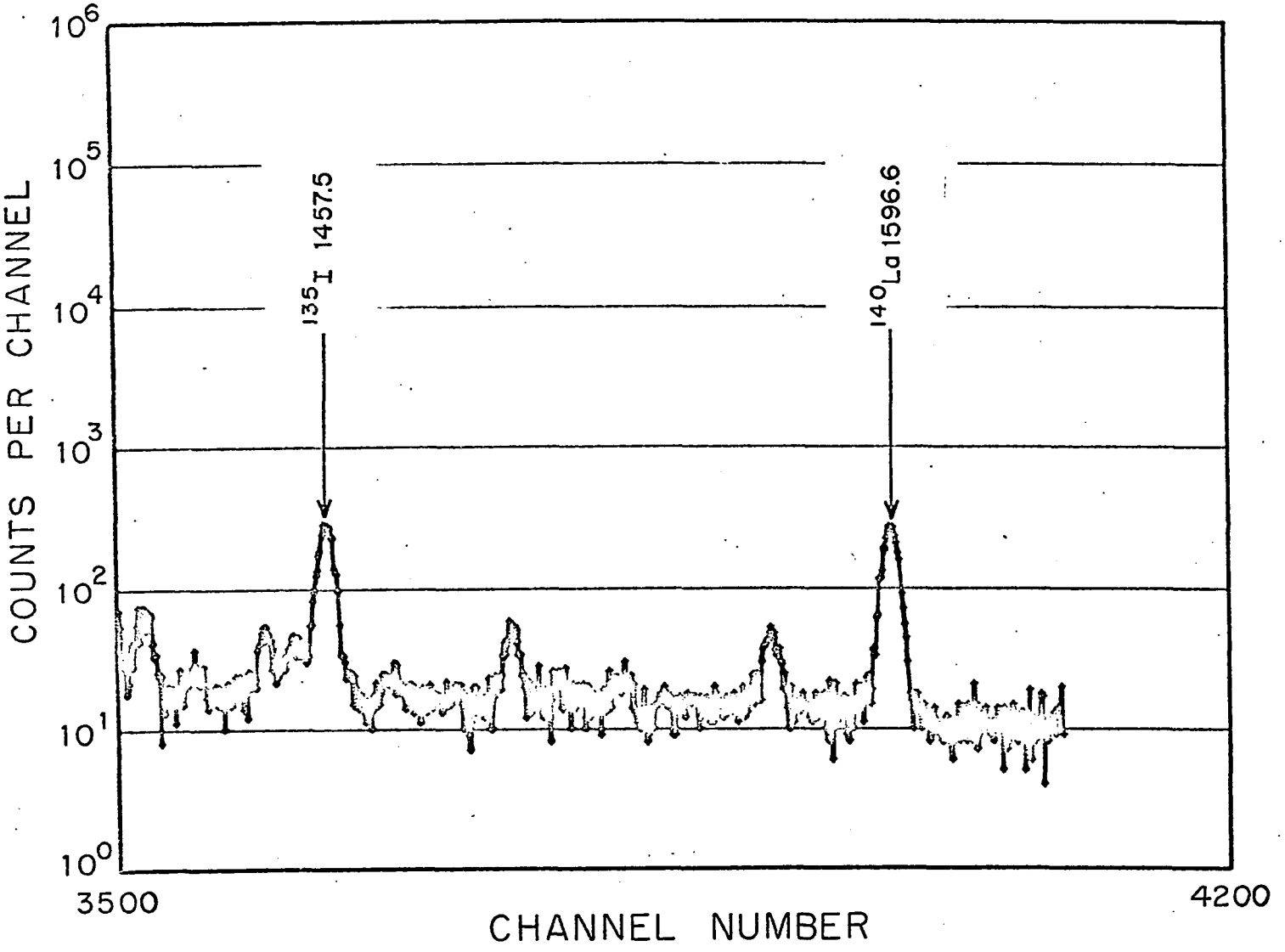

Fig. 12. ^{235}U gamma-ray spectrum at 1 day after irradiation, Continued.

Fig. 13. Gross fission product gamma-ray spectrum from the thermal fission of ^{235}U, taken at 7 days after irradiation.

The irradiation time was 20 minutes and the 4096 channel data is presented in six frames. The energy range of the data is approximately 40 to 1600 keV.

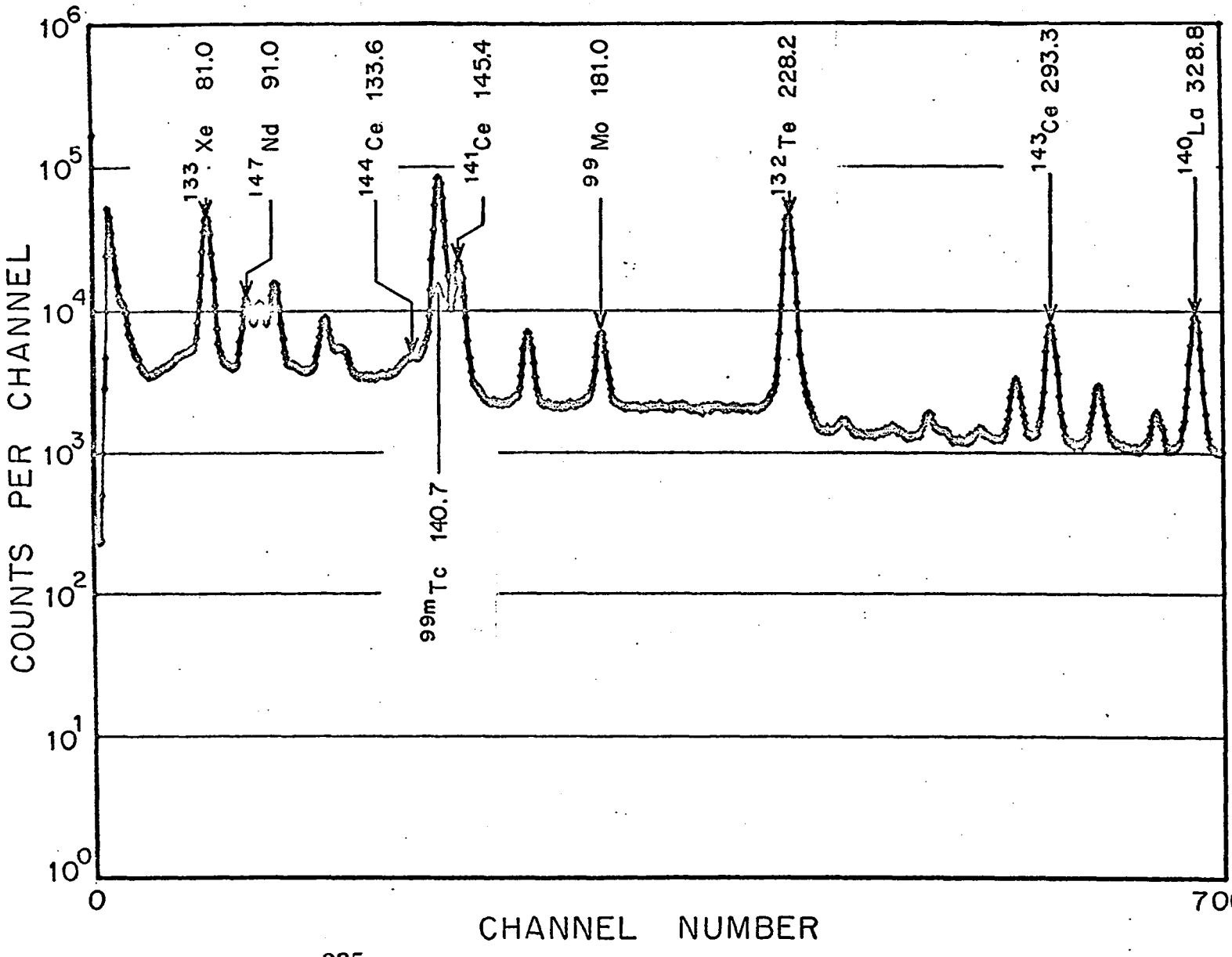

Fig. 13. ^{235}U gamma-ray spectrum at 7 days after irradiation.

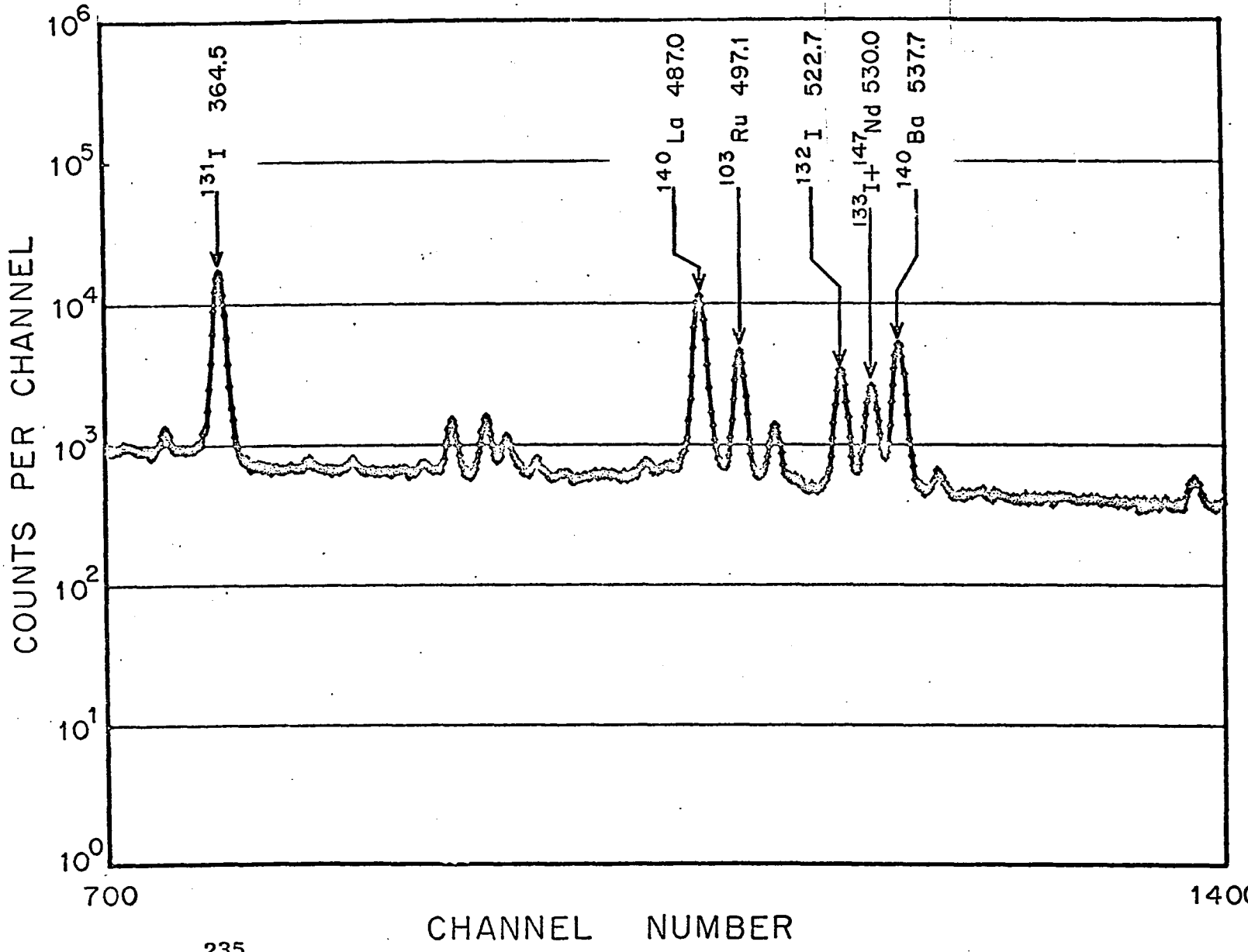

Fig. 13. ^{235}U gamma-ray spectrum at 7 days after irradiation, Continued.

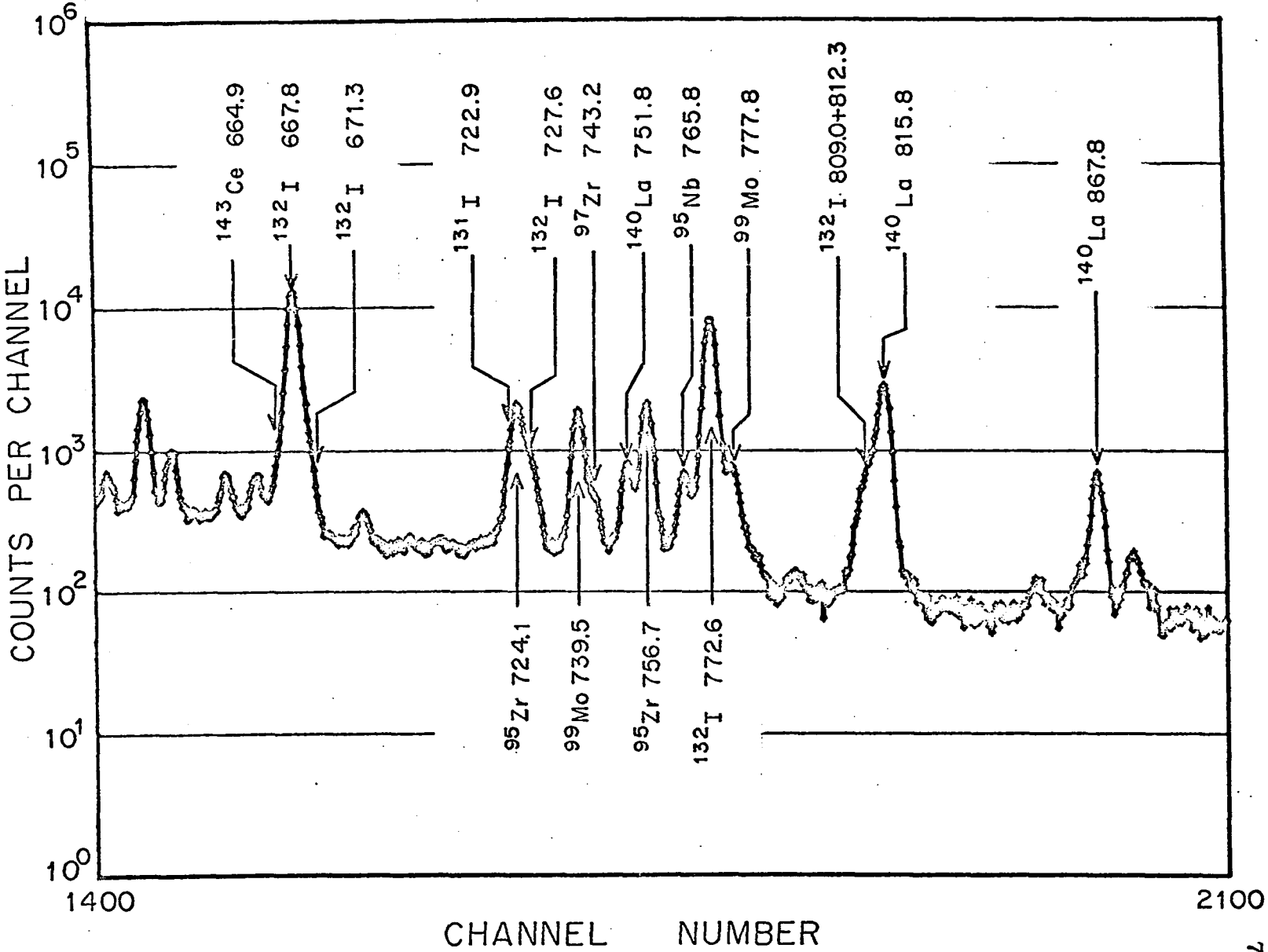

Fig. 13. ^{235}U gamma-ray spectrum at 7 days after irradiation, Continued.

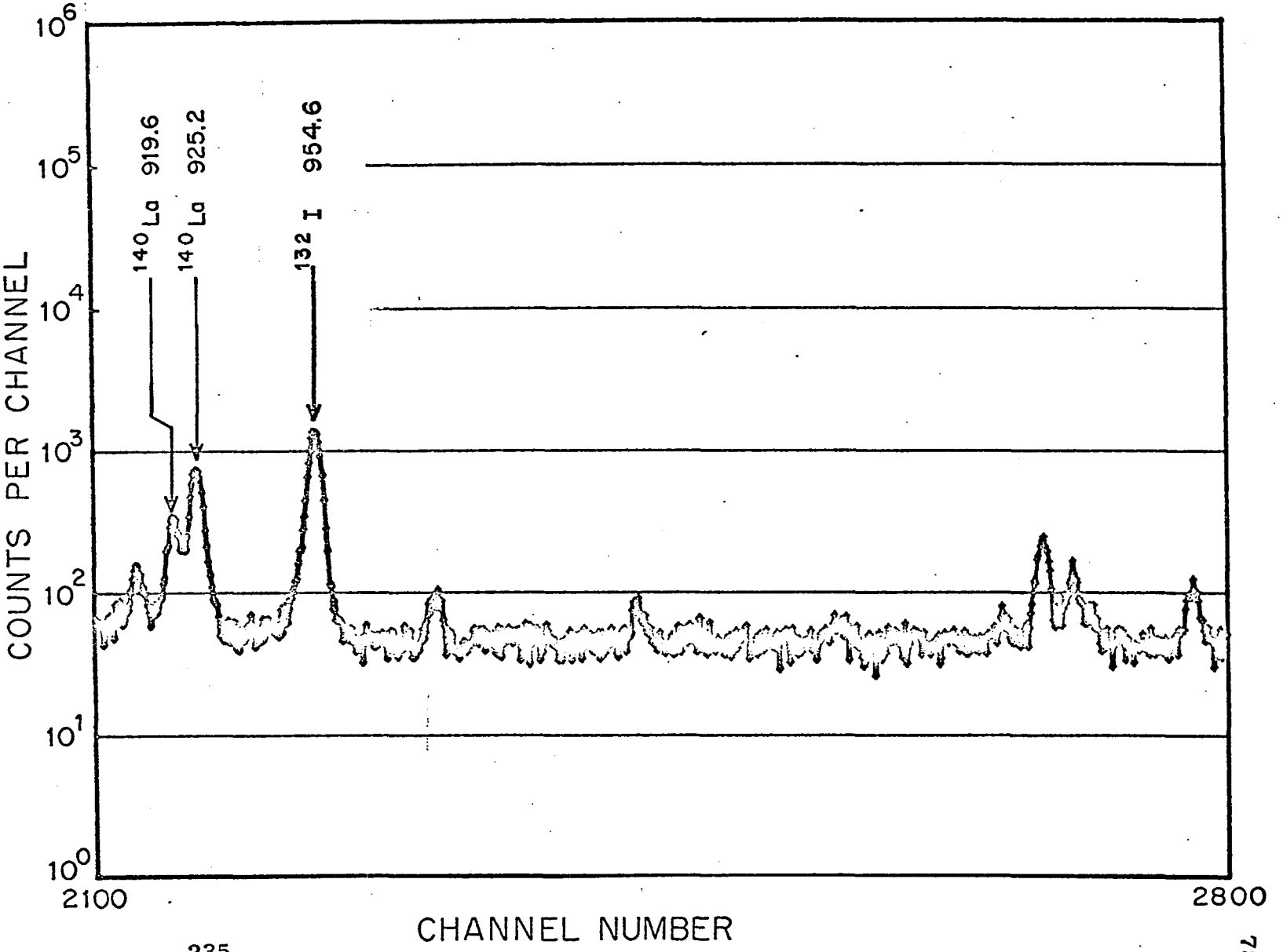

Fig. 13. ^{235}U gamma-ray spectrum at 7 days after irradiation, Continued.

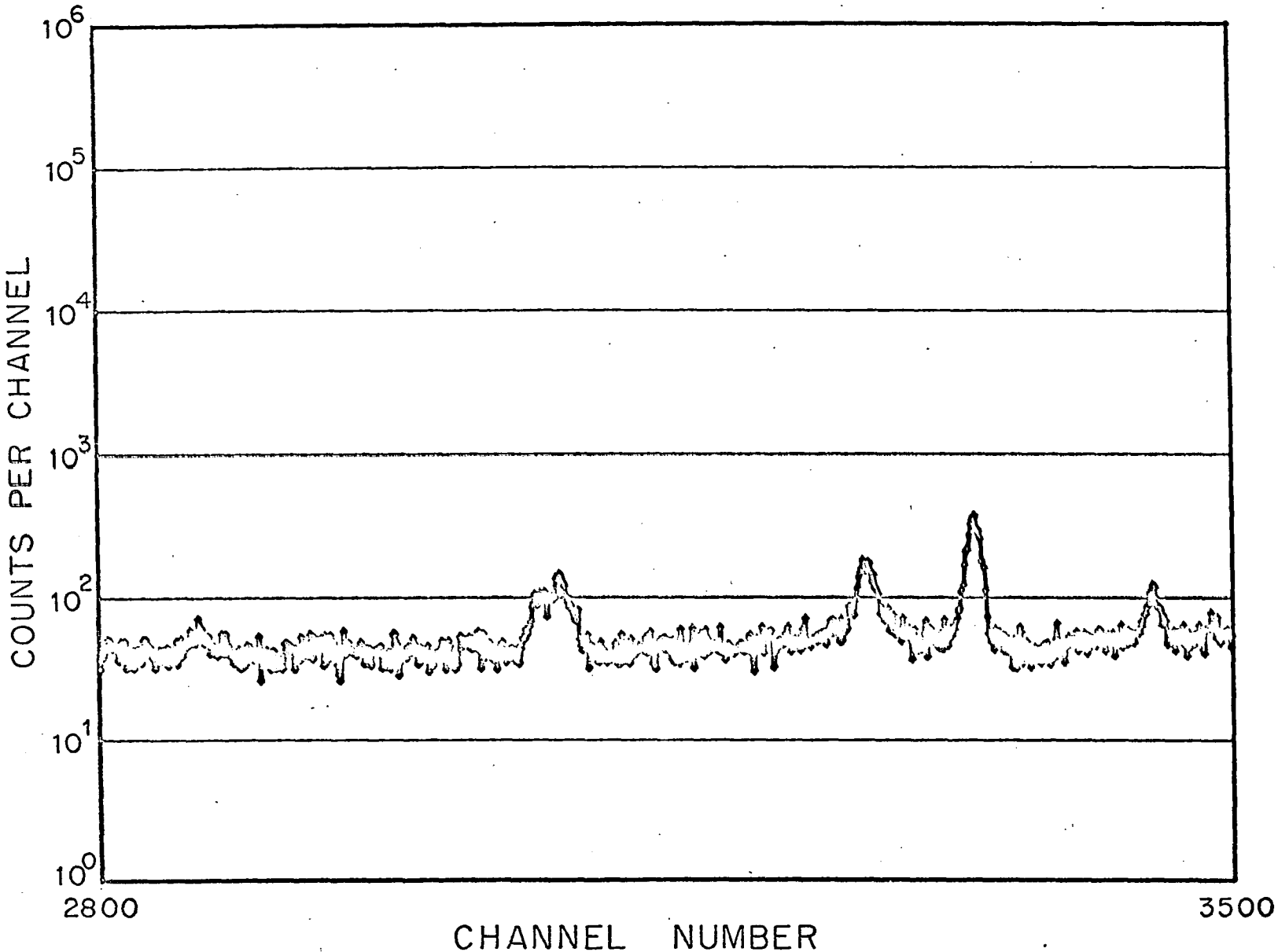

Fig. 13. ^{235}U gamma-ray spectrum at 7 days after irradiation, Continued.

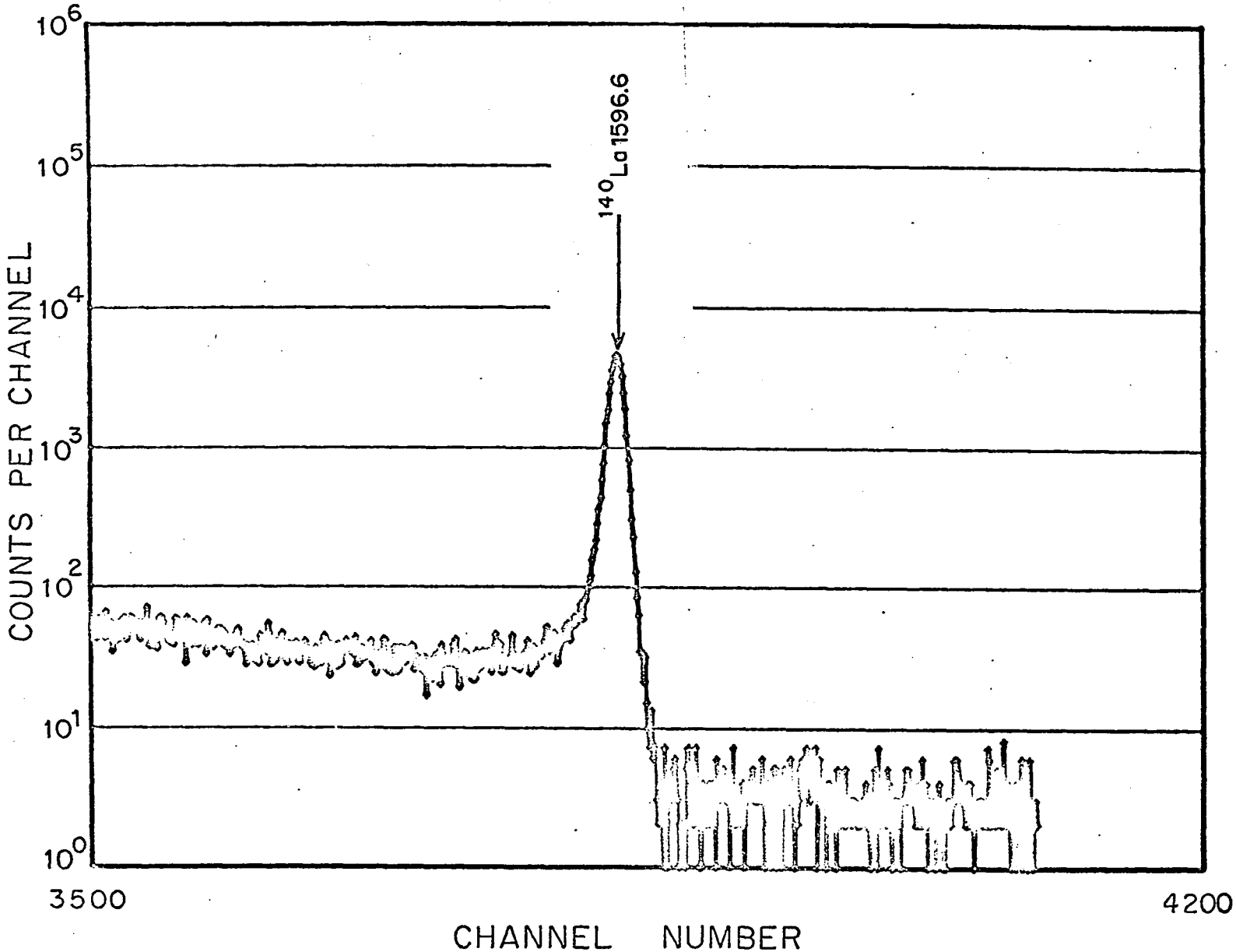

Fig. 13. ^{235}U gamma-ray spectrum at 7 days after irradiation, Continued.

Fig. 14. Gross fission product gamma-ray spectrum from the thermal fission of ^{235}U, taken at 57 days after irradiation.

The irradiation time was 20 minutes and the 4096 channel data is presented in six frames. The energy range of the data is approximately 40 to 1600 keV.

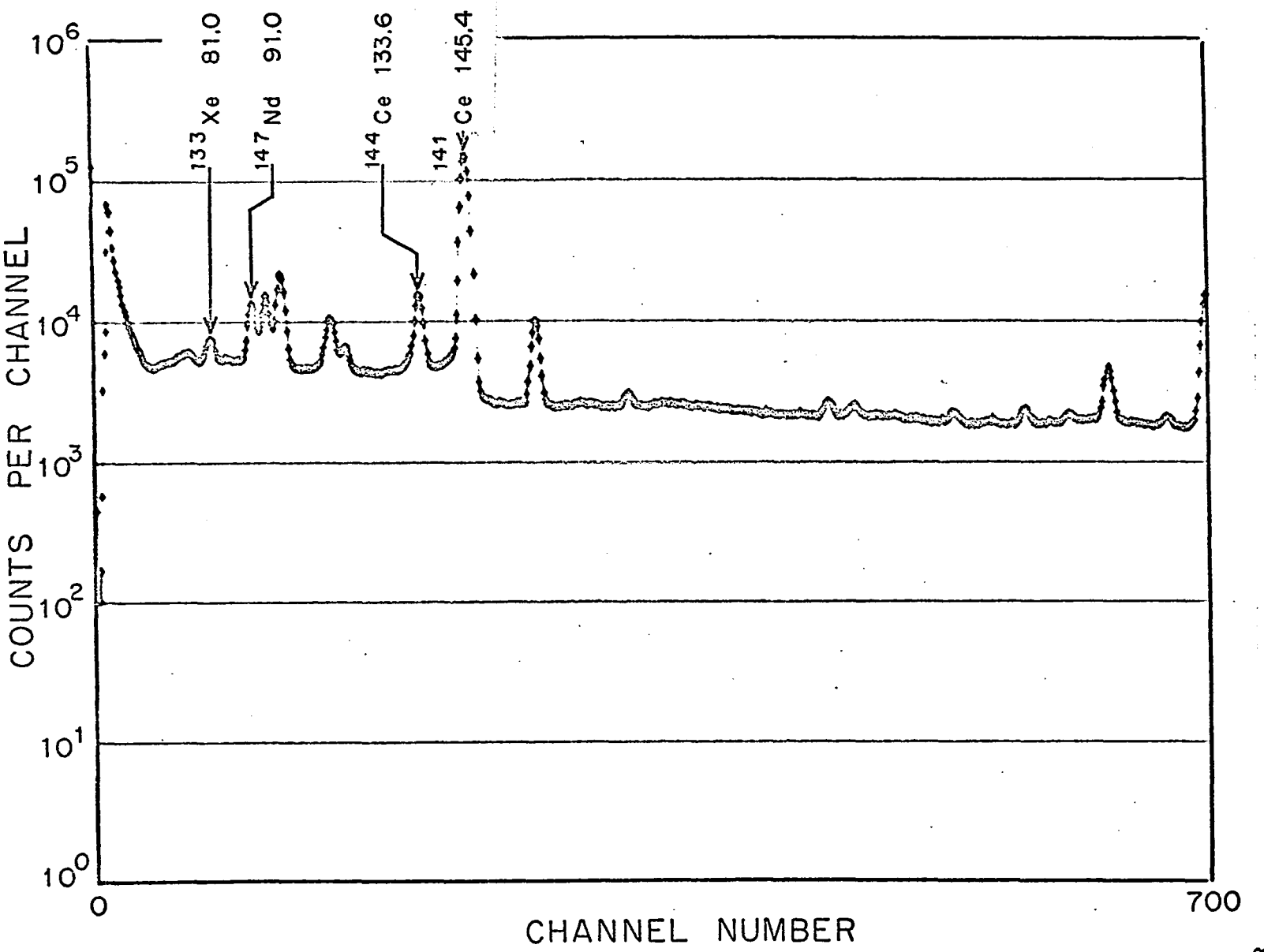

Fig. 14. ^{235}U gamma-ray spectrum at 57 days after irradiation.

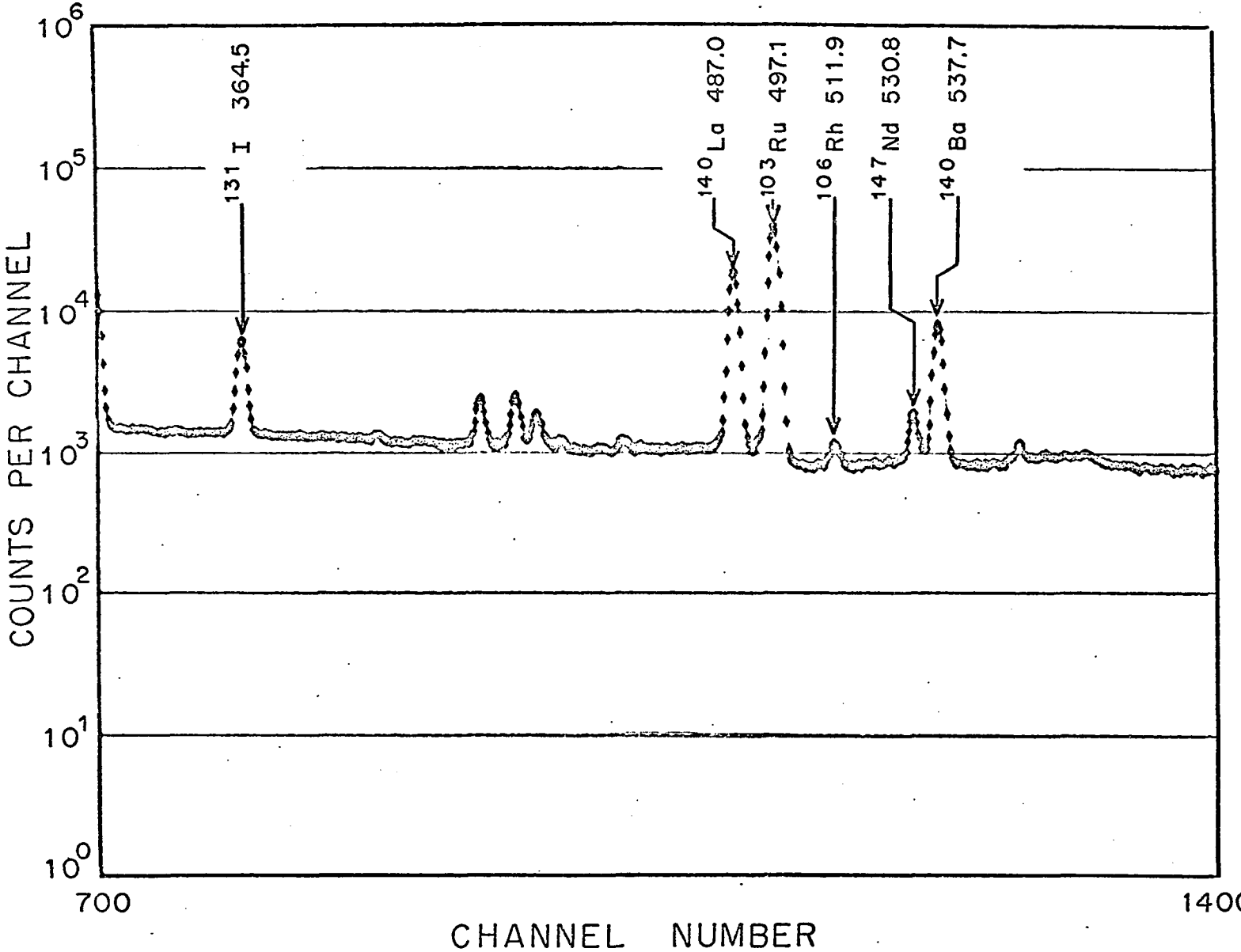

Fig. 14. ^{235}U gamma-ray spectrum at 57 days after irradiation, Continued.

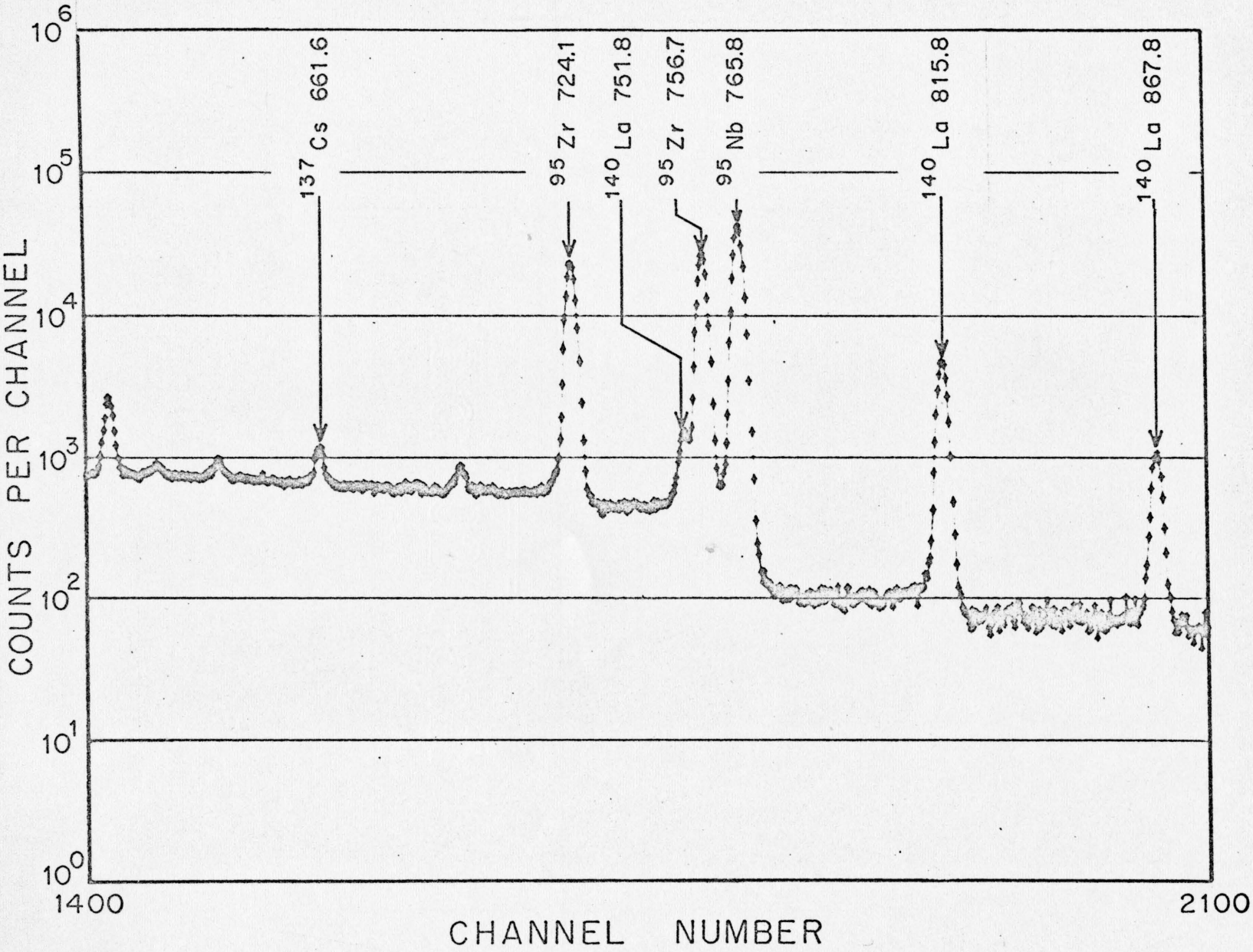

Fig. 14. ^{235}U gamma-ray spectrum at 57 days after irradiation, Continued.

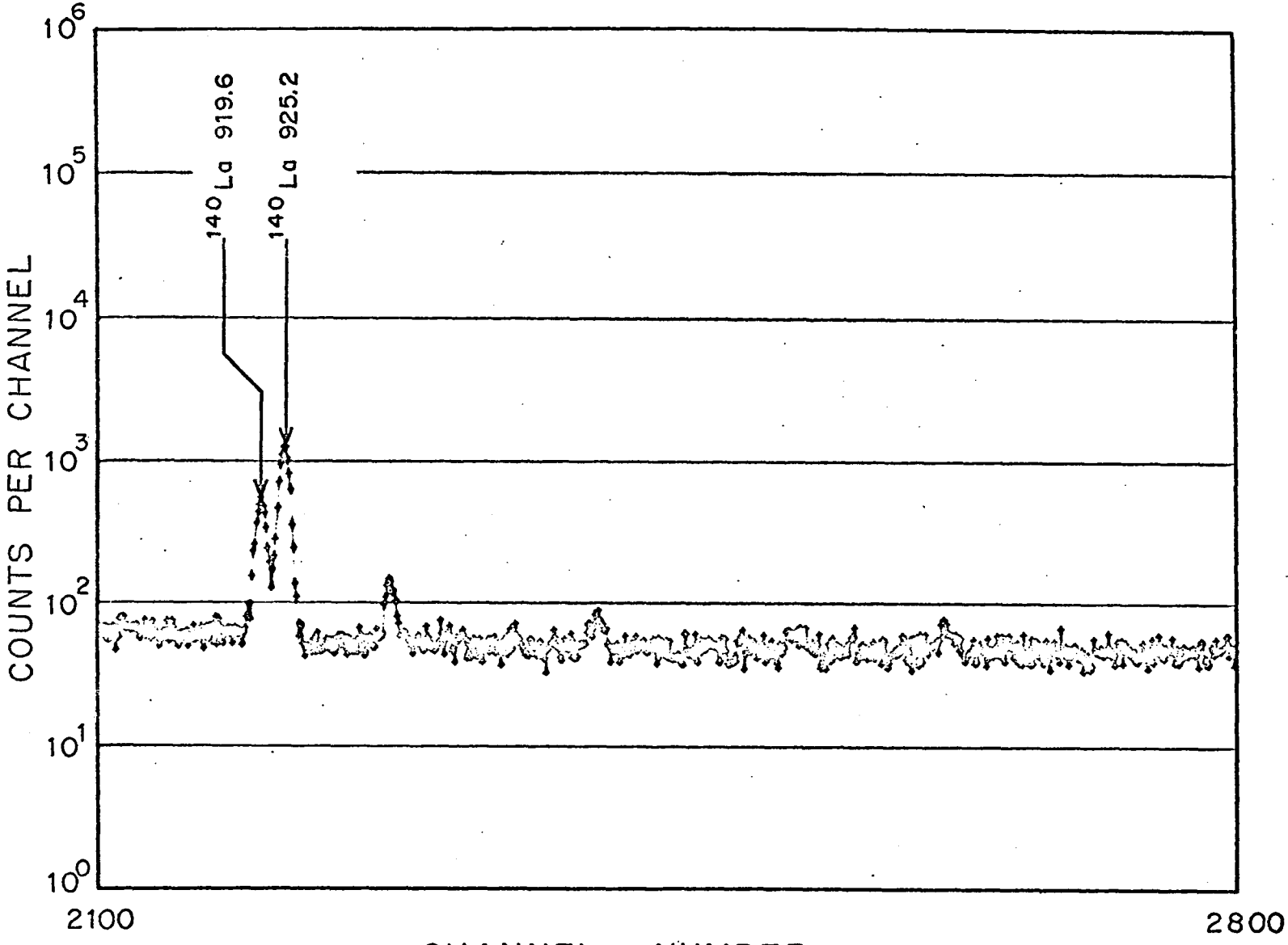

Fig. 14. ^{235}U gamma-ray spectrum at 57 days after irradiation, Continued.

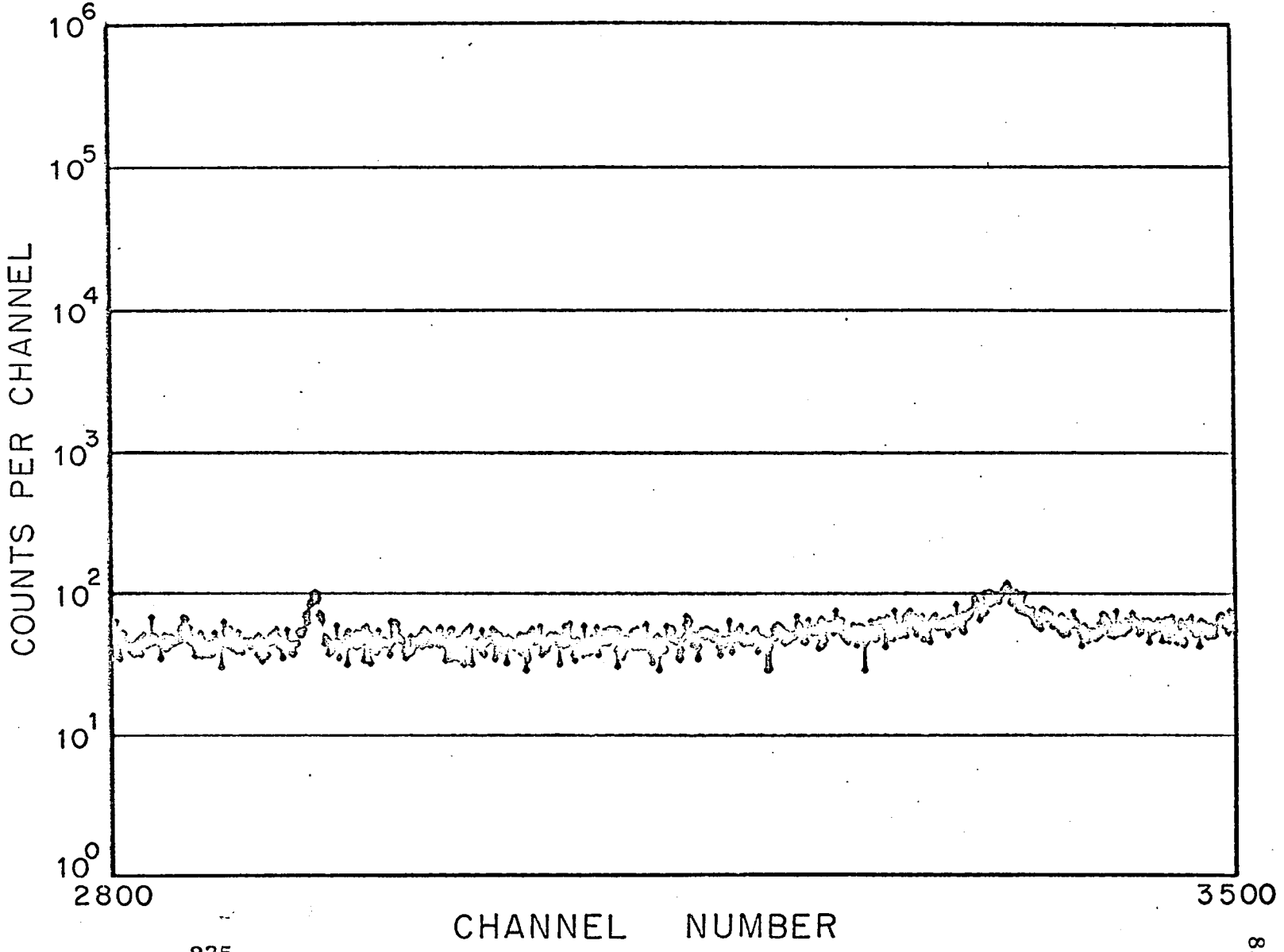

Fig. 14. ^{235}U gamma-ray spectrum at 57 days after irradiation, Continued.

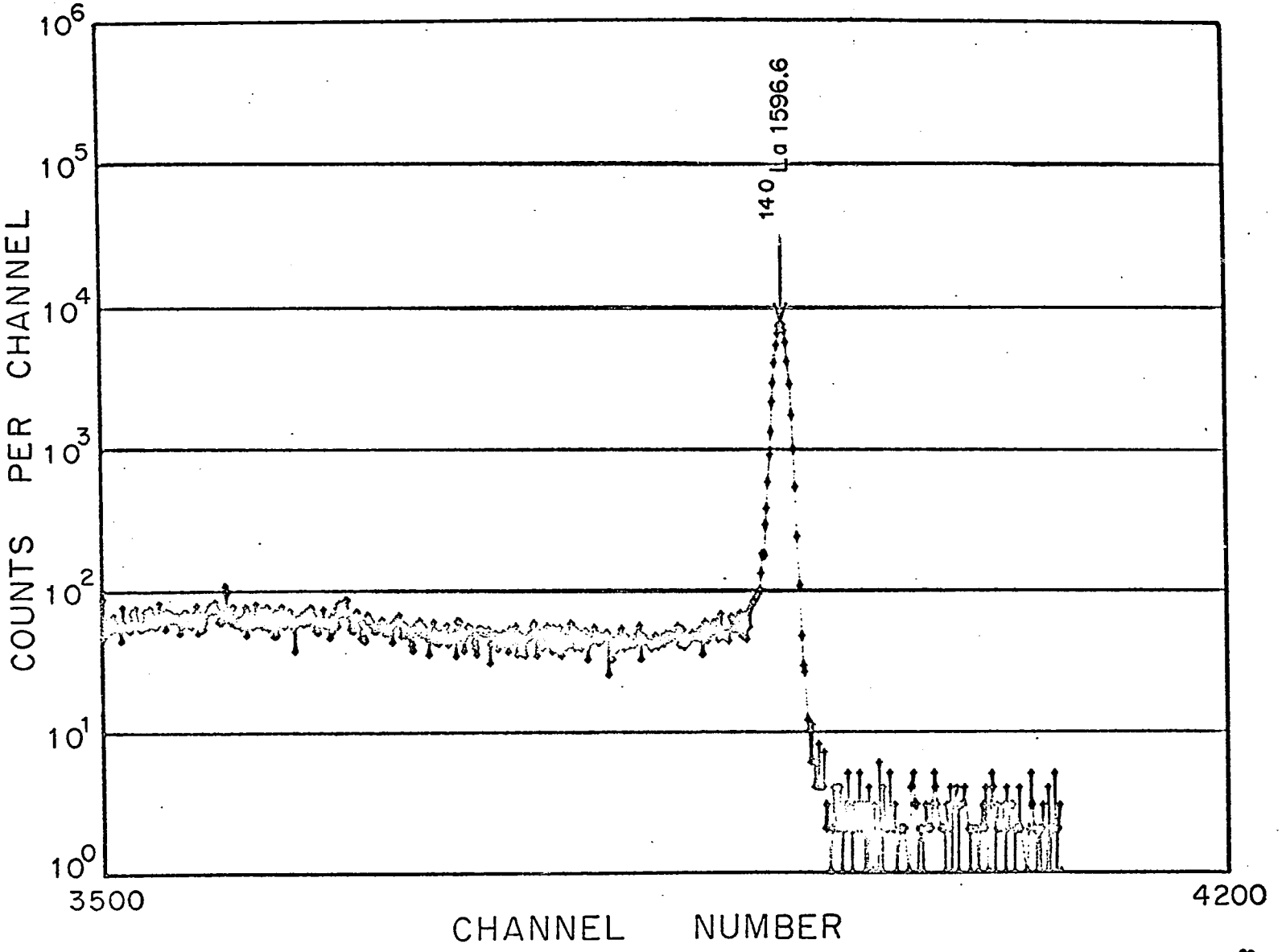

Fig. 14. ^{235}U gamma-ray spectrum at 57 days after irradiation, Continued.

APPENDIX C

DECAY SCHEME AND Ge(Li) DETECTOR EFFICIENCY DATA

Listed in Table 3 are the half-lives and gamma-ray intensities used in the yield calculations. For those fission products with parents which have non-negligible half-lives, all significant half-lives are given. Stated uncertainties in the intensity data are based on the values obtained from the literature search performed for this work.

All half-life and gamma-ray intensity data published prior to 1966 are summarized in a book by Lederer, Hollander, and Perlman (1967). For many nuclides investigated in this work there were also several more recent references. For clarity these references are given in an abbreviated form in Table 8. This compact form includes the first two letters of the last name of the author and the last two numerals of the year of publication. A letter following the two numerals is used to differentiate between publications in the same year by authors with last names beginning with the same two letters.

Given in Table 9 are the Ge(Li) detector efficiency data which were used in the least squares spline fitting and interpolation program. For the benefit of future users of this detector a careful measurement of the source-detector

Table 3. Half-life and absolute gamma-ray intensity data.

NUCLIDE	$T_{\frac{1}{2}}$	E_γ(keV)	I_γ(%)	REFERENCES
^{85m}Kr	4.4 h	151.1	74.0 ± 2.0	
^{87}Kr	78.0 m	402.4	59.0 ± 2.0	Ho67,On68,Ly68, Bo69
^{88}Kr	2.8 h	196.1	38.1 ± 2.2	Ly68
^{91}Sr	9.85 h	652.9	15.0 ± 1.8	
		749.8	27.0 ± 2.0	
		1024.3	30.0 ± 2.0	
^{91m}Y	50.5 m	555.6	58.0 ± 1.8	
^{92}Sr	2.71 h	1384.0	90.0 ± 1.0	
^{93}Y	10.2 h	266.7	6.3 ± 0.6	Ar69
^{95}Zr	65.5 d	724.1	48.5 ± 0.5[a]	Br66,Fo69,Go66a
		756.7	51.5 ± 0.5[a]	
^{95}Nb	35.15 d	765.8	100.0 ± 0.2	Re68
^{97}Zr	17.0 h	743.2	93.5 ± 0.3	Si68,Ho70,Ta69a
^{97}Nb	73.74 m	657.9	98.4 ± 0.2	Gr68a,Ho70,Is69, Si69,Ta69a
^{99m}Tc	66.7 h	140.7	81.8 ± 0.4	Re68,Va68,Ba69
	6.04 h			
^{103}Ru	39.5 d	497.1	88.0 ± 0.5	Po66,Ma66,Ra69, Zo69
^{106}Rh	367.0 d	511.9	21.0 ± 0.8	Go66a,Ve67,Od69

Table 3, Continued.

NUCLIDE	$T_{\frac{1}{2}}$	E_γ(keV)	I_γ(%)	REFERENCES
^{131}I	30.0 h	364.5	82.0 ± 0.6	Be67b,Yt67,Re68
	8.05 d			
^{132}Te	78.0 h	228.3	90.2 ± 1.0	An64,Fr66,Go66a
^{132}I	2.30 h	667.7	99.7 ± 0.2	An64,He69
		772.9	75.0 ± 1.8	
^{133}I	55.0 m	529.8	90.0 ± 1.0	Pa67,Mc68,Re68
	20.9 h			
^{133}Xe	5.27 d	81.0	36.5 ± 0.9	Go66a,Al68a
^{134}I	41.8 m	847.0	95.2 ± 0.4	Be67a,Ta69b,Wi69
	52.5 m	884.1	64.8 ± 0.7	
^{135}I	6.70 h	1260.4	23.5 ± 2.0	
^{135}Xe	9.17 h	249.6	91.1 ± o.4	Al68a,Op68
^{137}Cs	30.2 y	661.6	85.1 ± 0.4	Re68
^{138}Cs	32.2 m	1435.0	74.0 ± 2.0	Ca68
^{139}Ba	9.5 m	165.8	21.9 ± 0.9	Hi68,Be69,Su69
	82.9 m			
^{140}La	12.8 d	1596.6	95.5 ± 0.3	Hu66,Go66a,Ka67, Ba68,Re68
	40.3 h			
^{141}Ce	33.0 d	145.5	48.5 ± 1.2	Go66a
^{142}La	11.0 m	641.1	48.0 ± 1.1	Wa67b,Al68b
	92.0 m			

Table 3, Continued.

NUCLIDE	$T_{\frac{1}{2}}$	E_γ(keV)	I_γ(%)	REFERENCES
^{143}Ce	14.0 m	293.3	46.3 ± 4.0	Go66a,Wa67c, Gr68b,Me68
	33.5 h			
^{144}Ce	284.9 d	133.5	10.8 ± 0.9	Wa67d,Re68
^{147}Nd	11.1 d	91.1	27.6 ± 0.5	Ca67,Do67,Wa67e
		530.7	12.6 ± 0.5	
^{149}Nd	2.3 m	211.3	23.7 ± 1.5	Ba66,Go66b,He66
	1.73 h			

a. Intensity values were determined in this work.

Table 4. Absolute Ge(Li) efficiency data.

SOURCE	ENERGY(keV)	EFFICIENCY(10^6)
^{241}Am(IAEA)	59.5	23.02 ± 0.49
^{166m}Ho	80.3	54.5 ± 1.6
^{57}Co(IAEA)	122.0	67.58 ± 1.41
^{154}Eu	123.1	66.6 ± 1.6
^{166m}Ho	184.2	61.3 ± 1.0
^{166m}Ho	215.6	50.4 ± 1.0
^{154}Eu	248.0	43.1 ± 0.8
^{133}Ba	276.3	37.1 ± 1.1
^{203}Hg(IAEA)	279.2	36.94 ± 0.37
^{166m}Ho	279.6	36.85 ± 0.55
^{166m}Ho	299.3	34.4 ± 0.6
^{133}Ba	302.8	34.4 ± 1.0
^{133}Ba	356.0	25.6 ± 0.9
^{166m}Ho	364.9	26.0 ± 0.6
^{133}Ba	383.9	23.0 ± 0.8
^{166m}Ho	410.5	23.2 ± 0.5
^{166m}Ho	450.7	20.3 ± 0.4
^{22}Na(IAEA)	511.0	17.24 ± 0.17
^{166m}Ho	569.6	16.2 ± 0.4
^{154}Eu	591.7	14.5 ± 0.3
^{137}Cs(IAEA)	661.6	12.78 ± 0.15
^{166m}Ho	669.5	12.70 ± 0.16

Table 4, Continued.

SOURCE	ENERGY(keV)	EFFICIENCY(10^6)
^{166m}Ho	710.6	11.97 ± 0.17
^{154}Eu	722.3	11.79 ± 0.25
^{166m}Ho	751.5	11.78 ± 0.22
^{154}Eu	756.8	11.25 ± 0.24
^{166m}Ho	777.9	10.97 ± 0.22
^{166m}Ho	809.5	10.24 ± 0.10
^{166m}Ho	829.7	10.00 ± 0.08
^{54}Mn(IAEA)	834.8	9.80 ± 0.06
^{154}Eu	873.2	9.58 ± 0.16
^{88}Y(IAEA)	898.0	9.46 ± 0.14
^{154}Eu	996.3	8.18 ± 0.17
^{154}Eu	1004.8	8.30 ± 0.17
^{60}Co(IAEA)	1173.2	6.99 ± 0.05
^{154}Eu	1274.4	6.42 ± 0.07
^{22}Na(IAEA)	1274.5	6.42 ± 0.07
^{60}Co(IAEA)	1332.5	6.11 ± 0.04
^{88}Y(IAEA)	1836.1	4.34 ± 0.05

calibration distance was made. A value of 94.75 ± 0.05 cm was determined for the perpendicular distance from the front surface of the cryostat extension to the radioactive source.

APPENDIX D

DERIVATION OF RADIOACTIVE DECAY EQUATIONS

The rate of change of the number of atoms of a fission product during a sample irradiation can be written as

$$\frac{dN_1(t)}{dt} = Y_1 \Sigma_f \phi V - \lambda_1 N_1(t) \qquad \text{(D-1)}$$

where

$N_1(t)$ is the number of atoms of type 1 at time t,

Σ_f is the average macroscopic fission cross section,

ϕ is the volume averaged neutron flux in the sample,

V is the volume of the sample,

λ_1 is the decay constant of fission product N_1, and

Y_1 is the probability per fission for the production of fission product N_1.

The assumptions inherent in Eq. (D-1) are: that there is no loss of N_1 due to neutron absorption, that there is negligible burnup of the fissionable atoms initially present, and that N_1 has no parent decaying and creating atoms of type 1. As discussed in Chapter 2, this last assumption may be relaxed if the half-lives of the isobars prior in the decay chain are all negligible compared to the half-life of N_1.

For this case, Y_1 is the cumulative chain yield of fission product N_1.

Now $\Sigma_f \phi V$ is just the fission rate occurring in the sample. Therefore, if the flux is not a function of time one can write

$$Y_1 \Sigma_f \phi V = Y_1 \left(\frac{P}{t_1}\right)$$

where P is the total number of fissions which were induced in the sample and t_1 is the irradiation time. Thus Eq. (D-1) can be written as

$$\frac{dN_1(t)}{dt} = Y_1 \left(\frac{P}{t_1}\right) - \lambda_1 N_1(t). \qquad \text{(D-2)}$$

For the initial condition, $N_1(0) = 0$, this equation can be solved by standard techniques to obtain the number of atoms of N_1 present at the end of the irradiation,

$$N_1(t_1) = \frac{YP}{\lambda_1 t_1}\left(1-e^{-\lambda_1 t_1}\right). \qquad \text{(D-3)}$$

The rate of change of atoms of type 1 after irradiation is

$$\frac{dN_1(t)}{dt} = -\lambda_1 N_1(t). \qquad \text{(D-4)}$$

Using the initial condition, $N_1(t_1)$, as given by Eq. (D-3), the number of atoms of N_1 for times greater than t_1 is given by the solution of Eq. (D-4),

$$N_1(t \geq t_1) = \frac{YP}{\lambda_1 t_1}\left(1-e^{-\lambda_1 t_1}\right) e^{-\lambda_1 (t-t_1)}. \qquad \text{(D-5)}$$

The absolute number of atoms of N_1 which decay in the time interval (t_3-t_2) after irradiation can be expressed as

$$N_1(t_2) - N_1(t_3) = \int_o^{t_3-t_2} \lambda_1 N_1(t_2) e^{-\lambda_1 t}\, dt. \qquad \text{(D-6)}$$

For a detector efficiency, ϵ, percent gamma-ray emission per decay, I_γ, self-absorption factor, f_{SA}, and detection system live time, T_L, the counts recorded in the detector in the time interval (t_3-t_2) are

$$C = Y_1 P \frac{\epsilon I_\gamma f_{SA} T_L}{t_1 \lambda_1} \left(1-e^{-\lambda_1 t_1}\right) e^{-\lambda_1 (t_2-t_1)} \left(1-e^{-\lambda_1 (t_3-t_2)}\right). \qquad \text{(D-7)}$$

Now, if fission product N_1 has a daughter, N_2, which has a negligible independent yield, then the rate of change of daughter atoms during irradiation can be expressed as

$$\frac{dN_2(t)}{dt} = Y_1\left(\frac{P}{t_1}\right) + \lambda_1 N_1(t) - \lambda_2 N_2(t). \qquad \text{(D-8)}$$

The solution to Eq. (D-8) for the initial condition, $N_2(0) = 0$, and for an irradiation of duration t_1 is

$$N_2(t_1) = Y_1\left(\frac{P}{t_1}\right) \left\{ \frac{\lambda_1}{\lambda_2(\lambda_1-\lambda_2)} \left(1-e^{-\lambda_2 t_1}\right) - \frac{1}{\lambda_1-\lambda_2} \left(1-e^{-\lambda_1 t_1}\right) \right\}. \qquad \text{(D-9)}$$

The rate of change of daughter atoms after the irradiation can be written as

$$\frac{dN_2(t)}{dt} = \lambda_1 N_1(t) - \lambda_2 N_2(t).$$

This equation can be solved for the initial condition, $N_2(t_1)$, as given by Eq. (D-9) with the result

$$N_2(t \geq t_1) = Y_1\left(\frac{P}{t_1}\right)\left\{\frac{\lambda_1}{\lambda_2(\lambda_1-\lambda_2)}\left(1-e^{-\lambda_2 t_1}\right)e^{-\lambda_2(t-t_1)}\right.$$

$$\left. - \frac{1}{\lambda_1-\lambda_2}\left(1-e^{-\lambda_1 t_1}\right)e^{-\lambda_1(t-t_1)}\right\}. \qquad \text{(D-10)}$$

The absolute number of daughter atoms which decay in the time interval (t_3-t_2) after irradiation can be expressed as

$$N_2(t_2) - N_2(t_3) = \int_{t_2}^{t_3} \lambda_2 N_2(t)\,dt. \qquad \text{(D-11)}$$

The detector counts recorded for a gamma-ray from the decay of the daughter are then

$$C = Y_1 P \frac{\epsilon I_\gamma f_{SA} T_L}{t_1}\left\{\frac{\lambda_2}{\lambda_1(\lambda_2-\lambda_1)}\left(1-e^{-\lambda_1 t_1}\right)\left(e^{-\lambda_1(t_2-t_1)}\right.\right.$$

$$\left. - e^{-\lambda_1(t_3-t_1)}\right) - \frac{\lambda_1}{\lambda_2(\lambda_2-\lambda_1)}\left(1-e^{-\lambda_2 t_1}\right)\left(e^{-\lambda_2(t_2-t_1)}\right.$$

$$\left.\left. - e^{-\lambda_2(t_3-t_1)}\right)\right\}. \qquad \text{(D-12)}$$

REFERENCES

Alexander, P. and J. P. Lau, "Nuclear Structure in ^{133,135}Xe and ^{133,135}Cs," Nucl. Phys. A121, 612 (1968).

Alvager, T., R. A. Naumann, R. F. Petry, G. Sidenius, and T. D. Thomas, "On-Line Studies of Mass-Separated Xenon Fission Products," Phys. Rev. 167, 1105 (1968).

Andersson, G., G. Rudstam, and G. Sorenson, "Decay Data on some Xe, I, and Te Isotopes," Arkiv Fysik 28, 37 (1964).

Arad, B., J. Butler, W. V. Prestwich, and K. Fritze, "Level Scheme of ^{93}Zr," Nucl. Phys. A131, 137 (1969).

Ardisson, G., "Sur la Desintegration de L'iode 132," Compt. Rend. Serie C, 1999 (1967).

Backlin, A., S. G. Malmskog, and H. Solhed, "Transitions, Lifetimes, and Levels in ^{149}Pm," Arkiv Fysik 34, 495 (1966).

Baer, H. W., J. J. Reidy, and M. L. Wiedenbeck, "The Decay of ^{140}La to Levels in ^{140}Ce," Nucl. Phys. A113, 33 (1968).

Berg, V., K. Fransson, and C. E. Bemis, "The Decay of ^{134}Te," Arkiv Fysik 37, 203 (1967).

Berzins, G., M. E. Bunker, and J. W. Starner, "The Decay Scheme of ^{139}Ba," Nucl. Phys. A124, 294 (1969).

Beyer, L. M. and W. H. Kelly, "Conversion Electron Measurements of Transitions Following the Beta Decay of ^{131}Te," Nucl. Phys. A104, 274 (1967).

Bocquet, J. P., R. Brissot, J. Crancon, J. A. Pinston, F. Schussler, and A. Moussa, "Desintegration du ^{87}Kr," Nucl. Phys. A125, 613 (1969).

Boggs, J. V., "Gamma-Ray Spectra of Fission Products from ^{235}U as a Function of Time after Fission," Ph. D. Dissertation, Univ. of Oklahoma (1966).

Brashandy, E. and N. Ibrahiem, "Nuclear Level Structure of ^{99}Tc," Z. Physik 219, 337 (1969).

Broman, L. and S. Boreving, "An Investigation of the Decay ^{95}Zr-^{95}Nb-^{95}Mo," Arkiv Fysik 34, 259 (1966).

Canty, M. J. and R. D. Connor, "The Decay of ^{147}Nd," Nucl. Phys. A104, 35 (1967).

Carlsson, G. C., W. C. Schick,Jr., W. L. Talbert,Jr., and K. F. Wohn, "Half-Lives of some Short-Lived Mass-Separated Gaseous Fission Products and Their Daughters," Nucl. Phys. A125, 267 (1969).

Case, K. M., F. de Hoffmann, and G. Placzek, "Introduction to the Theory of Neutron Diffusion, Volume I," Los Alamos Scientific Laboratory (1953).

Dalton, G. R. and R. K. Osborn, "Flux Perturbations by Thermal Neutron Detectors," Nucl. Sci. Eng. 9, 198 (1961).

Dougan, P. W. and B. Erlandsson, "On the Decay of ^{147}Nd," Z. Physik 207, 105 (1967).

Foin, C., J. Oms, J. Blachot, and J. Crancon, "Etude de la Desintegration ^{95}Zr-^{95}Nb," Nucl. Phys. A123, 513 (1969).

Fransson, K. and C. E. Bemis,Jr., "The Decay of ^{132}Te and Levels in Odd ^{132}I," Nucl. Phys. 78, 207 (1966).

Goldstein, G. and S. A. Reynolds, "Specific Activities and Half-Lives of Common Radionuclides," Nucl. Data A1, 435 (1966).

Gopinathan, K. P. and R. M. Singru, "Levels of ^{149}Pm from the Decay of ^{149}Nd," Phys. Rev. 150, 985 (1966).

Gordon, G. E., J. W. Harvey, and H. Nakahara, "Measuring Fission Spectra with Semiconductor Detectors," Nucleonics 24, 62 (1966).

Graeffe, G. and A. Siivola, "The Decay of ^{97}Nb," Nucl. Phys. A109, 380 (1968).

Gregory, P. R., L. Schellenberg, Z. Sujkowski, and M. W. Johns, "Levels in ^{143}Pr Populated in the Decay of ^{143}Ce," Can. J. Phys. 46, 2797 (1968).

Hanna, G. C., "The Depression of Thermal Neutron Flux and Density by Absorbing Foils," Nucl. Sci. Eng. 11, 338 (1961).

Hanna, G. C., "The Neutron Flux Perturbation Due to an Absorbing Foil; A Comparison of Theories and Experiments," Nucl. Sci. Eng. 15, 325 (1963).

Helmer, R. G. and L. D. McIsaac, "Decay of ^{149}Nd," Phys. Rev. 143, 923 (1965).

Henck, M. R. and A. Gizon, "Coefficients de Conversion Interne de Transitions de Basse Energie de la Desintegration ^{132}I-^{132}Xe," Compt. Rend. Serie B, 337 (1969).

Hill, J. C. and M. L. Wiedenbeck, "Levels in the N=82 Nucleus ^{139}La Populated in ^{139}Ba Decay," Nucl. Phys. A119, 53 (1968).

Hofstetter, K. J. and T. T. Sugihara, "Decay of ^{97}Ru, ^{97}Zr, and ^{97}Nb," Nucl. Phys. A140, 658 (1970).

Holm, G., "Energy Levels in the Single Closed Shell Nucleus ^{87}Rb," Arkiv Fysik 34, 433 (1967).

Huguet, M., H. Forest, and C. Ythier, "Sur L'etude du Rayonnement Gamma de Haute Energie au Moyen d'un Spectrometre a Paires a Haute Resolution," Compt. Rend. Serie B, 79 (1966).

Karlsson, S. E., B. Svahn, H. Pettersson, G. Mamsten, and E. Y. Aisenberg, "The Decay of ^{140}La," Nucl. Phys. A100, 113 (1967).

Knobeloch, G. W., "Precision Assay by Fission Counting," EANDC Conf., Brussels (1965).

Lederer, C. M., J. M. Hollander, and I. Perlman, Table of Isotopes, Sixth Edition, John Wiley and Sons, Inc., 1967.

Lisman, F. L., W. J. Maeck, J. E. Rein, R. E. Foster,Jr., R. M. Abernathy, J. E. Delmore,Jr., W. A. Emel, M. E. Kussy, R. E. McAtee, and G. D. Workman, "Burnup Determination of Nuclear Fuels, Project Report for the Quarter April 1 - June 30, 1968 and Final Report," IN-1277, Idaho Nuclear Corporation (1969).

Lycklama, H., N. P. Archer, and T. J. Kennett, "Beta Decay of ^{87}Kr, ^{88}Kr, and ^{88}Rb," Can. J. Phys. 47, 393 (1969).

Malenfant, R. E., "QAD; A Series of Point-Kernel General-Purpose Shielding Programs," LA-3573, Los Alamos Scientific Laboratory (1967).

Malm, H. L., "Improvements in Large Volume Coaxial Germanium Spectrometers," IEEE Trans. Nucl. Sci. NS-13, 285 (1966).

Manthuruthil, J. C., H. J. Hennecke, and C. R. Cothern, "Internal-Conversion-Electron Study of the Decay of ^{103}Ru," Phys. Rev. 165, 1363 (1968).

McIsaac, L. D., "Levels in ^{133}I from the Decay of ^{133m}Te and ^{133g}Te," Phys. Rev. 172, 1253 (1968).

Megli, D. G., V. R. Potnis, and C. E. Mandeville, "Nuclear States of ^{143}Pr," Nucl. Phys. A107, 117 (1968).

Moore, B. M., "Short-Lived Delayed Gamma-Ray Emission from Fast Fission of Plutonium," LA-4257, Los Alamos Scientific Laboratory (1969).

Murri, E. L. and R. L. Heath, "Nuclear Technology Branch Yearly Progress Report for Period Ending June 30, 1968," IN-1218, Idaho Nuclear Corporation (1968).

Odru, P. P., "Rapports D'embranchments et Intensites Relatives des Gamma du ^{105}Rh et du ^{106}Rh," Rad. Acta 12, 64 (1969).

Onega, R. J. and W. B. Carpenter, "The Decay Scheme of ^{87}Kr," Nucl. Phys. A137, 211 (1969).

Op de Beeck, J. P. and W. B. Walters, "Decay of 9.2-h ^{135}Xe," J. Inorg. Nucl. Chem. 30, 2881 (1968).

Parsa, B., G. E. Gordon, and W. B. Walters, "Decay of the 55 min and 12 min ^{133}Te Isomers," Nucl. Phys. A101, 674 (1967).

Potnis, V. R., E. B. Nieschmidt, C. E. Mandeville, L. D. Ellsworth, and G. P. Agin, "Some Nuclear States of ^{103}Rh," Phys. Rev. 146, 883 (1966).

Povelites, J. G., "Preparation of Thin Films of UO_2 and PuO_2 by Vacuum Evaporation," AERE-R 5097, Atomic Energy Research Establishment (1965).

Profio, A. E., H. M. Antunez, and D. L. Huffman, "The Neutron Spectrum from a Fission Source in Graphite," Nucl. Sci. Eng. 35, 91 (1969).

Raeside, D. E., J. J. Reidy, and M. L. Wiedenbeck, "The Levels of ^{103}Ru," Nucl. Phys. A134, 347 (1969).

Rao, P. V. and R. W. Fink, "Levels in ^{106}Pd from Decay of 8.5 d ^{106m}Ag, 24 min ^{106g}Ag and 30 sec ^{106g}Rh," Nucl. Phys. A103, 385 (1967).

Reynolds, S. A., J. F. Emery, and E. I. Wyatt, "Half-Lives of Radionuclides - III," Nucl. Sci. Eng. 32, 46 (1968).

Rider, B. F., C. P. Ruiz, J. P. Peterson,Jr., and F. R. Smith, "A Survey and Evaluation of Thermal Fission Yields for U-235, Pu-239, U-233, and Pu-241," GEAP-5356, General Electric (1967).

Sanders, W. M. and D. M. Holm, "An Analytical Method for Unfolding Gamma-Ray Spectra," LA-4030, Los Alamos Scientific Laboratory (1969).

Siivola, A. and G. Graeffe, "The Decay of ^{97}Zr," Nucl. Phys. A109, 369 (1968).

Singh, B., R. J. Cox, A. H. Kukoc, J. D. King, and H. W. Taylor, "A Study of the Gamma Rays Emitted by ^{97}Nb," Nucl. Phys. A129, 104 (1969).

Storm, E. and H. I. Israel, "Photon Cross Sections from 0.001 to 100 MeV for Elements 1 through 100," LA-3753, Los Alamos Scientific Laboratory (1967).

Sunier, J. W. and J. Berthier, "Shape Factor and Directional Correlation Measurements in the First Forbidden Beta Decay of ^{139}Ba," Nucl. Phys. A124, 673 (1969).

Taff, L. M., "Nuclear Decays of ^{97}Zr and ^{97}Nb," Ph. D. Dissertation, Iowa State University (1969).

Takekoshi, E., H. Umezawa, and T. Suzuki, "A Study of the Decay Scheme of ^{134}I," Nucl. Phys. A134, 493 (1969).

Tisinger, R. M., Group W-7, Los Alamos Scientific Laboratory, Personal Communication (1970).

Tomitaro, I. and U. Kaoru, "Collected Papers on Disintegration Studies of Short-Lived Nuclides," JAERI 1178, Japan Atomic Energy Research Institute (1969).

Van Eijk, C. W. E., B. Van Nooijen, F. Schutte, S. M. Brahmaver, J. H. Hamilton, and J. J. Pinajian, "The Decay of ^{99}Mo," Nucl. Phys. A121, 440 (1968).

Wahl, A. C., A. E. Norris, R. A. Rouse, and J. C. Williams, "Products from Thermal-neutron Induced Fission of ^{235}U - A Correlation of Charge and Mass Distribution Data," (to be published).

Way, K., "A = 142," Nucl. Data, B2-1, 1 (1967).

Way, K., "A = 143," Nucl. Data, B2-1, 25 (1967).

Way, K., "A = 144," Nucl. Data, B2-1, 47 (1967).

Way, K., "A = 147," Nucl. Data, B2-4, 35 (1967).

Winn, W. G. and D. G. Sarantites, "Ge(Li) - Ge(Li) Study of the ^{134}I Decay," Phys. Rev. 184, 1188 (1969).

Ythier, C. and G. Ardisson, "Sur le Rayonnement Gamma de L'iode 131," Compt. Rend. Serei C, 944 (1967).

Zoller, W. H., E. S. Macias, M. B. Perkal, and W. B. Walters, "Decay of 40 d ^{103}Ru and 17 d ^{103}Pd to Levels in ^{103}Rh," Nucl. Phys. A130, 293 (1969).